CONF-831259--1

CONF-831259--1

DE84 004458

FUSION-RELEVANT BASIC RADIATION EFFECTS — THEORY AND EXPERIMENT

L. K. MANSUR, W. A. COGHLAN, K. FARRELL, L. L. HORTON,
E. H. LEE, M. B. LEWIS, AND N. H. PACKAN

Metals and Ceramics Division
Oak Ridge National Laboratory
Oak Ridge, Tennessee 37831 (USA)

PAPER PRESENTED AT THE

JAPAN-U.S. WORKSHOP ON FUSION REACTOR MATERIALS

Tsukuba, Japan

December 5-7, 1983

DISCLAIMER

This report was prepared as an account of work sponsored by an agency of the United States Government. Neither the United States Government nor any agency thereof, nor any of their employees, makes any warranty, express or implied, or assumes any legal liability or responsibility for the accuracy, completeness, or usefulness of any information, apparatus, product, or process disclosed, or represents that its use would not infringe privately owned rights. Reference herein to any specific commercial product, process, or service by trade name, trademark, manufacturer, or otherwise does not necessarily constitute or imply its endorsement, recommendation, or favoring by the United States Government or any agency thereof. The views and opinions of authors expressed herein do not necessarily state or reflect those of the United States Government or any agency thereof.

MASTER

DISTRIBUTION OF THIS DOCUMENT IS UNLIMITED

FUSION-RELEVANT BASIC RADIATION EFFECTS — THEORY AND EXPERIMENT[1]

L. K. Mansur, W. A. Coghlan,[2] K. Farrell, L. L. Horton, E. H. Lee
M. B. Lewis, N. H. Packan

Metals and Ceramics Division
Oak Ridge National Laboratory
Oak Ridge, TN 37831 (USA)

A summary is given of results of the basic radiation effects program at Oak Ridge National Laboratory, which are relevant to fusion reactor materials applications. The basic radiation effects program at ORNL is a large effort with the dual objectives of understanding the atomic and microstructural defect mechanisms underlying radiation effects and of determining principles for the design of radiation resistant materials. A strength of this effort is the parallel and integrated experimental and theoretical approaches in each major research area. The experimental effort is active in electron microscopy, ion irradiations and ion-beam techniques, neutron irradiations, surface analysis and in other areas. The theoretical effort is active in developing the theory of radiation effects for a broad range of phenomena and in applying it to the design and interpretation of experiments and to alloy design.

Because of the importance and lack of mechanistic understanding of anticipated materials problems in fusion reactors, a significant fraction of this work is aimed at the special characteristics, materials, and phenomena to be encountered there. A brief review is given of recent work in the following areas:

- Theory of Helium Effects on Microstructural Evolution
- Swelling and Precipitation Behavior in Complex Phosphorous-Containing Austenitic Alloys — Critical Number of Gas Atoms and Alloy Design
- The Effects of Helium and Its Mode of Introduction on the Microstructural Response of a Stable Austenitic Alloy
- Through-Range Ion Damage in Nickel
- Neutron Irradiation Studies of Iron and Vanadium
- Pulsed Irradiation Effects in a Stable Austenitic Alloy
- Pulsed Irradiation Effects in an Unstable Austenitic Alloy

---

[1]Research sponsored by the Division of Materials Sciences, U.S. Department of Energy under contract W-7405-eng-26 with the Union Carbide Corporation.

[2]Present address: Arizona State University, Tempe, AZ 85281.

By acceptance of this article, the publisher or recipient acknowledges the U.S. Government's right to retain a nonexclusive, royalty-free license in and to any copyright covering the article.

THEORY OF HELIUM EFFECTS ON MICROSTRUCTURAL EVOLUTION

Helium is a special transmutation product which produces significant changes in the radiation effects response of metals and alloys. Helium exerts strong effects on the critical radius for bias-driven swelling, and when a critical number of helium atoms, n_g^*, is present in a cavity the critical size for bias-driven growth is reduced to zero. Analytical expressions have been derived for n_g^* and for the minimum critical radius, r_c^{c*}. These relations allow easy exploration of the effects of variables of interest such as temperature, dose rate, sink strength and bias on the critical quantities. At high temperatures the critical number of gas atoms is large and the dose interval to the onset of bias-driven swelling is expected to be large and to be determined by the time taken to accumulate n_g^* gas atoms in cavities. Without helium at high temperatures the critical radius is large and therefore bias driven swelling would be difficult or impossible, because random fluctuations, which are ineffective at causing large size excursions, are then the only way to achieve bias-driven swelling.

It is also found that the critical number of gas atoms is quite sensitive to the dislocation sink strength. This implies that in a given material, bias-driven swelling will be "patchy," especially during the early stages of irradiation. Swelling will occur first in regions where n_g^* is lower because of the local dislocation density. This also implies that the time to the onset of bias-driven swelling will vary substantially from one material to another where the dislocation densities are different, when other differences in the materials are

accounted for. The critical number of gas atoms and minimum critical radius concepts also predict the existence and some properties of bimodal cavity size distributions in the presence of helium. These conclusions based on theory are in good agreement with a wide range of experimental observations.

In addition, the kinetics of the growth stage of cavity swelling is affected by helium. Helium generally increases the concentrations of cavities. This may have two effects. One is to move the system toward cavity dominated point defect absorption. In the extreme this reduces the dose exponent of swelling to less than unity. A detailed exposition of the effect of the balance of sink strengths on the dose exponents and magnitudes of swelling has been given previously. The other effect is to introduce a second population of cavities — those cavities hovering at their stable radius corresponding to their contained number of gas atoms ($n_g < n_g^*$). These stable cavities absorb vacancies and interstitials, which recombine there. The swelling behavior corresponding to the bias-driven cavities is thereby altered in magnitude and dose dependence.

Helium also interacts with radiation-induced precipitation. Two aspects are of great interest. The first concerns preferential nucleation of cavities on precipitate matrix interfaces. It has been demonstrated that helium induces small cavities on the interfaces. These cavities may reach critical size or number of gas atoms earlier and grow more rapidly than cavities in the matrix. The more rapid growth rate has been predicted theoretically and observed experimentally to be due to point defect collection on the precipitate-matrix interface and channelled diffusion to the cavity. The second effect concerns the effect of helium on radiation-affected precipitation. In experiments on stainless steels under both neutron and ion irradiation helium has been shown to suppress precipitation of phases which would

otherwise occur, thus changing the volume fraction of precipitate, the sequence of precipitation reactions, and the mixture of phases present. The mechanism we believe responsible for these changes centers on the increase of cavity sink strength for solutes associated with helium. More sites for solute segregation dilute the segregation at each site. Since the number of solute atoms is fixed this leads to lesser local enrichments and may eliminate the possibility of precipitation reactions with higher solubility limits.

SWELLING AND PRECIPITATION BEHAVIOR IN COMPLEX PHOSPHOROUS-CONTAINING AUSTENITIC ALLOYS — CRITICAL NUMBER OF GAS ATOMS AND ALLOY DESIGN

Austenitic stainless steel type alloys are potential candidate alloys for magnetic fusion reactor and breeder reactor structural materials applications. Their swelling and creep behavior is strongly influenced by the precipitate phases that occur during irradiation. The alloys investigated here are phosphide-forming austenitic stainless steels irradiated with neutrons in EBR-II and with 4 MeV Ni-ions and 0.2–0.4 MeV helium ions in the ORNL dual-ion beam Van de Graaff. The principal effect of the addition of phosphorous and silicon in this alloy was to enhance the formation of a needle-shaped iron phosphide precipitate during irradiation. It was found that cavity formation did not occur when a high density of phosphide precipitates formed during irradiation. The unusual swelling resistance of this material to high doses prompted an investigation of the distribution of injected helium using high resolution electron microscopy. It was found that the precipitate-matrix interfaces serve as sites for the nucleation of a very fine dispersion of helium bubbles.

This observation suggests to us that high precipitate-matrix interfacial area may be associated with swelling suppression, and a mechanism to explain the experimental observation is proposed. The mechanism is based on a requirement that emerges from the theory of cavity swelling — the occurrence of bias driven swelling under the present conditions requires as a prerequisite the accumulation of a critical number of gas atoms in each cavity. Thus the higher the precipitate-matrix interfacial area of these precipitates, the smaller is the number of gas atoms in each cavity, as required by dilution of a fixed amount of helium. As a consequence, it takes longer to accumulate the critical number of gas atoms where the number of cavities is larger. Theoretical calculations based on expressions we derived previously have been carried out using measured microstructural information obtained from the experiment. The theoretical calculations predict the gross features of the experimental observations, swelling

is observed only in the case where the critical number of gas atoms has been accumulated. This work provides a clear principle for alloy design for swelling resistance, based on the introduction of a fine and stable precipitate particle distribution.

THE EFFECTS OF HELIUM AND ITS MODE OF INTRODUCTION ON THE MICROSTRUCTURAL RESPONSE OF A STABLE AUSTENITIC ALLOY

The availability of a dual-accelerator ion bombardment facility has permitted well-controlled investigation of the role of helium and its mode of introduction. A series of experiments has been conducted on P7, a simple austenitic alloy analogous to type 316 stainless steel, of composition Fe-17Cr-16.7Ni-2.5Mo (wt %), using a fusion-realm 20 appm He/dpa injection rate and doses from 1 to 70 dpa. The material swells readily and remains single-phase under irradiation, thus permitting a focus on microstructural, as contrasted with micro-compositional, effects of helium on cavity nucleation and growth.

In this material, bombardment at 900 K with 4 MeV nickel ions alone gives rise to the largest (but fewest) cavities and the highest swelling. Simultaneous injection of 0.2–0.4 MeV He^+ ions yields somewhat more numerous but smaller cavities and swelling. If the equivalent quantity of helium is instead preimplanted before the damage-producing bombardment, a much different and bimodal rather than unimodal cavity size distribution results. Conducting the preimplantation at room temperature (rather than at 900 K) yields the smallest and most numerous cavities and the lowest swelling. In the context of the theory of swelling, such preimplantation conditions cause the cavities to become the dominant point defect sink. At the extensive cavity surface area, swelling remains low even out to 70 dpa, because vacancy-interstitial recombination is enhanced, since nearly all defects of either type are absorbed at the cavities. The presence of the bimodal cavity size distribution implies that a barrier exists to the growth of some, or, for room temperature preimplantation, most of the cavities. We have been able to show that the small cavities are quasi-bubbles and that the largest of them are just below the critical size for bias-driven void growth predicted by theory.

Bombardments conducted over the full temperature range for swelling in this material revealed upward shifts of about 50K in both the upper temperature limit for swelling and the temperature for peak swelling. Again these results were found to be consistent with theoretical expectations. Introducing the helium by simultaneous, dual beam injection enhanced swelling over the widest temperature range, whereas preimplanted helium seemed to strongly promote swelling only in a narrow temperature region. The dislocations were much less sensitive to helium, although preimplanted helium retarded somewhat the progression from dislocation loops to network.

From these experiments, we conclude that introducing helium by room temperature preimplantation overstimulates cavity nucleation and yields misleading microstructural and swelling results, especially at the high helium concentrations involved in simulated fusion first-wall conditions. Dual beam simultaneous injection of helium is in every way a preferable technique.

THROUGH-RANGE ION DAMAGE IN NICKEL

This work was done to demonstrate the effects of helium on cavity nucleation and swelling, and to experimentally verify some special aspects of ion bombardment damage microstructures predicted by the theory of radiation effects.

Targets of pure nickel were bombarded with 4 MeV Ni ions at 873 K (0.51 T_m) to a nominal peak damage level of 50 dpa. Helium was implanted from a second particle accelerator at an oscillating energy in the range 0.2 to 0.4 MeV which ensured that the helium distribution was superimposed on the peak heavy ion damage region. Helium implantation to a level of 1000 appm was done in two ways. In the first, the helium was preimplanted at room temperature prior to raising the specimen to elevated temperature for heavy ion bombardment. This was the common method of implanting helium before dual beam facilities were developed, and is still used for most HVEM irradiations. The second method was coimplantation simultaneously with the heavy ion bombardment at elevated temperature, which more closely reproduces the continuous generation of helium that occurs during neutron irradiation. Following heavy ion bombardment, the targets were electroplated with nickel, sectioned along the direction of the incident ion beam to expose the full-damage profile, and thinned for TEM examination. Examples of the results are shown and the quantitative cavity data are presented.

It is obvious from the results that helium considerably increases the concentrations of cavities and decreases their sizes, and that cold preimplanted helium is much more effective in these respects than is coimplanted helium. Furthermore, cold preimplanted helium reduces the level of swelling at most depths, whereas coimplanted helium generally increases the swelling. It is clear, too, that the measured

cavitational swelling penetrates significantly deeper than the displacement events predicted from the E-DEP-1 code, and that there is denuding of damage in a shallow region (<0.1 μm) at the target surface. There is also an unusual band of dislocations (not shown in figures) at a depth of about 2 μm, which is almost twice the predicted maximum depth for significant displacement events.

All of these observations are satisfactorily explained by radiation damage theory. The increases in cavity concentrations caused by helium are due to stabilization of clusters of vacancies by internal pressures of helium gas which oppose thermal evaporation of vacancies from the clusters and aid the clusters in attaining a critical size above which they can grow by bias-driven mode. These helium-assisted cavities are additional point defect recombination centers, which at the high concentrations overbalance the dislocation sink strength. Their presence in large numbers results in slower cavity growth rates and hence, smaller cavities. Low-temperature implantation of helium nucleates many more He-V clusters than does high temperature implantation. When this refinement of the cavities produces a sink strength that greatly exceeds the dislocation sink strength, the rate of swelling is decreased. The absence of damage structure in the near-surface regions is due to the efficiency of the surface as a point defect sink, leading to low point defect concentrations in that region. The penetration of cavity swelling to depths beyond the damage depth is caused by diffusional spreading of point defects from the damaged region, and has been predicted by the theory. The deep band of dislocations is attributed to stress relief of the swollen region.

NEUTRON IRRADIATION STUDIES OF IRON AND VANADIUM

Iron-based ferritic steels and vanadium-based alloys are currently being considered as structural materials for fusion reactors. This interest results in part from the low swelling and low activation characteristics of these materials as compared to austenitic steels. In order to better understand damage mechanisms, study of the temperature dependence of neutron-irradiation damage and the effects of the helium levels expected for fusion rectors is important. One method of studying the effects of high concentrations of helium on the development of damage microstructures in fission reactors involves doping with the isotope ^{10}B which has a large cross section for the thermal neutron reaction $^{10}B + n \rightarrow {}^{4}He + {}^{7}Li$.

In the present investigations, the irradiation temperature dependence of the damage microstructures in iron (2 appm ^{10}B), vanadium (<0.1 appm ^{10}B) and vanadium with boron carbide additions ($V\text{-}B_4C$, 3900 appm ^{10}B) has been studied. Disk specimens of these materials were irradiated in helium-filled capsules in the Oak Ridge Research Reactor to ~1 dpa. Both the flux and the irradiation temperature were accurately monitored. The temperature was controlled to within $\pm 5°$ of the selected irradiation temperature. Microstructural analyses were performed with JEM 100C (equipped with the AMG objective lens pole-piece for magnetic specimen observations), JEM 100CX and Philips EM 400T/FEG analytical electron microscopes operated at 120 keV.

Comparisons of the damage microstructures in vanadium and iron suggest significant differences in the damage evolution for these materials. Iron was more resistant to cavitational swelling than vanadium. While cavity formation was limited to 0.3–0.4 T_m in iron, cavities were observed in vanadium for all irradiation temperatures (0.2–0.36 T_m). The maximum swelling was lower for iron (0.07%) than for vanadium (0.1%). For the same homologous temperatures, the cavities were smaller and were present in higher concentrations in vanadium than in iron. The dislocation microstructures were also quite

different. For example, the Burgers vectors of dislocation loops were predominantly a<100> in iron and were a/2<111> in vanadium. The detailed microstructural descriptions of the damage in vanadium and iron provided by this study should aid in understanding the differences between the damage mechanisms for ferritic materials and other bcc alloys.

In the iron specimens, damage halos formed around boron-containing precipitates. In the V-B_4C specimens, the damage was homogeneously distributed, suggesting that the boron was in solution rather than in precipitates prior to the irradiation. The effect of helium on the damage microstructures was studied through comparisons of halo and non-halo regions in the iron specimens and of vanadium and V-B_4C. The helium formed during the irradiation from the transmutation of ^{10}B promoted cavity formation. The cavities in V-B_4C were more numerous than the cavities in vanadium for the same irradiation temperature. In both iron and vanadium, helium aided cavity formation at irradiation temperatures higher than the temperatures at which significant cavity formation occurred without helium. This effect is in agreement with the theoretical prediction of increased swelling at high temperatures when helium is present. In addition, in V-B_4C and in regions near the damage halos in iron, cavities were observed on grain boundaries. The above observations suggest that helium could have a deleterious effect on the properties of iron- and vanadium-based alloys used for fusion reactor applications. Further study with the helium concentrations expected for the fusion environment is required to more accurately evaluate these problems.

PULSED IRRADIATION EFFECTS IN A STABLE AUSTENITIC ALLOY

One characteristic of many fusion reactor designs, the sequences of "burn" periods interspersed by off times can be studied by interrupting (pulsing) the heavy ion and helium beams of a dual beam ion bombardment facility. Theoretical analyses show that pulsed irradiation is also a powerful tool for manipulating and dissecting microstructural evolution processes according to their different kinetics and relaxation times. We began our pulsing studies using a high purity austenitic alloy designated P7 (Fe-17 wt % Cr-16.7 Ni-2.5 Mo) that was familiar to us from previous helium effects work. This alloy swells readily and remains single-phase under irradiation to high dose. Bombardments were conducted using 4 MeV Ni^{++} ions to a dose of 10 dpa at a dose rate of 2×10^{-3} dpa/s. Helium (200 at. ppm) was introduced simultaneously ("coimplanted"), preimplanted at room temperature, or omitted. Bombardment temperatures were 843, 938, and 1023 K, spanning the swelling regime in this material. Pulsing schedules were either "slow" (60s on/60s off) or "fast" (1s on/1s off) with steady beam as a control.

A strong effect that pervades the observations is the profound influence of this amount of helium upon cavity formation. Helium refines the cavities by decreasing the sizes and increasing the number density, and it generates a distinct second component of small cavities leading to bimodal cavity size distributions. The effect of pulsing is both temperature and helium sensitive. At 843 K, any influence of fast or slow pulsing on either the cavities or dislocations was small. The significant pulsing effect at 938 K, near the peak swelling temperature, was the <u>lack</u> of refinement of the large cavities for either dual beam or preimplanted helium so that the cavities resembled those of the helium-free case. In comparable steady irradiations with helium, the number of cavities was increased and their size decreased as a result of the helium. Near the high temperature limit for swelling, 1023 K, pulsing suppressed all large

cavities. The populations of the small cavities were not greatly affected by pulsing at any temperature. The dislocation densities were generally insensitive to pulsing except for the helium preimplanted specimens at higher temperatures.

These effects can be explained in light of changes to the critical size above which cavities can grow by bias-driven vacancy acceptance. Promotion of any cavity from the subcritical to the bias-driven class can occur by random size fluctuations or by further gas accumulation. Pulsing could alter the first mechanism since the beam-off annealing intervals would sharply curtail any upward size fluctuations — increasingly so the higher the temperature. During annealing the cavities lose vacancies and therefore partially reverse their progress toward the critical size. In addition, the rate of movement of helium to traps and defect clusters could also vary between beam on and beam off conditions. The effects of pulsing on overall swelling were not major in P7 except at 1023 K, but the above changes to cavity sizes provide unique data for comparison with mechanistic interpretations.

PULSED IRRADIATION EFFECTS IN AN UNSTABLE AUSTENITIC ALLOY

Recent research on radiation effects in complex alloys has shown that phase instability as well as microstructure is sensitive to irradiation variables. During irradiation, major and minor solute elements, especially nickel and silicon are driven to segregate to point defect sinks by the inexorable fluxes of vacancies and interstitials. Such segregation eventually leads to phase transformations near sinks resulting in the appearance of Ni- and Si-rich phases such as G, γ' and to the less-enriched η-phase. The MC phase, which forms rapidly during thermal annealing or during the early part of an irradiation, competes with these phases for some of the same elements. Motivated by these results, the influence of pulsed irradiation, with and without simultaneous helium injection, has been explored in a low swelling, Ti-modified austenitic stainless steel. Irradiations with 4 MeV Ni-ions and 0.2–0.4 MeV He-ions were carried out at 950 K to doses of 1, 10, 40, and 70 dpa with a helium injection rate of 20 appm/dpa. Five irradiation conditions were used: (a) continuous irradiation with no helium injection, (b) 60 s on/off pulsed irradiations with no helium injection, (c) continuous irradiation with simultaneous helium injection, (d) 60 s on/off pulsed irradiation with simultaneous helium injection, and finally (e) 1 s on/off pulsed irradiation with simultaneous injection.

Compared to continuous irradiation, pulsing caused a decrease in the interstitial loop diameter at 1 dpa, although at higher doses the overall dislocation density was not affected. Pulsing and helium both promoted the stability of MC precipitates and retarded the subsequent G-phase formation; in some cases G-phase was suppressed and eta phase formed instead. Small bubble-like cavities were observed to grow into large voids after steady dual beam irradiation to 70 dpa. However, no large cavities were produced by pulsed irradiation to 70 dpa, and furthermore the size of the small cavities was somewhat reduced.

Our preliminary analysis indicates that current understanding of point defect kinetics and the evolution of microstructure and microcomposition can be extended to explain these results. During the beam-off periods, it appears that interstitial loops are vulnerable to erosion by unopposed vacancy fluxes; the phase stability criteria reverse to favor MC reconstruction and nickel/silicon thermal desegregation which retards G-phase evolution; and small cavities regress toward their equilibrium sizes as bubbles.

- Theory of Helium Effects on Microstructural Evolution

ORNL-WS-23542

HELIUM AFFECTS SWELLING THROUGH SEVERAL REACTION PATHWAYS

- CAVITY PRESSURIZATION
- MICROSTRUCTURAL SINK STRENGTH
- PHASE STABILITY AND LOCAL COMPOSITION
- POINT DEFECT AND ATOMIC TRANSPORT

Origin of Critical Cavity Radius

Cavity Growth Rate

$$\frac{dr_c}{dt} = \frac{\Omega}{r_c}\left[\underbrace{Z_v^c D_v C_v - Z_i^c D_i C_i}_{\text{Net Influx by Radiation and Thermal Generation}} - \underbrace{Z_v^c D_v C_v^e(r_c)}_{\text{Outflux by Thermal Emission}}\right]$$

Thermal Vacancy Concentration Near Cavity

$$C_v^e(r_c) = C_v^e \exp\left[-\left(P_g - \frac{2\gamma}{r_c}\right)\frac{\Omega}{kT}\right]$$

At elevated T, influx and outflux terms become comparable. There is a cavity radius

$$r_c^{crit} \text{ for which } \frac{dr_c}{dt} = 0$$

ORNL-DWG 83C-9337

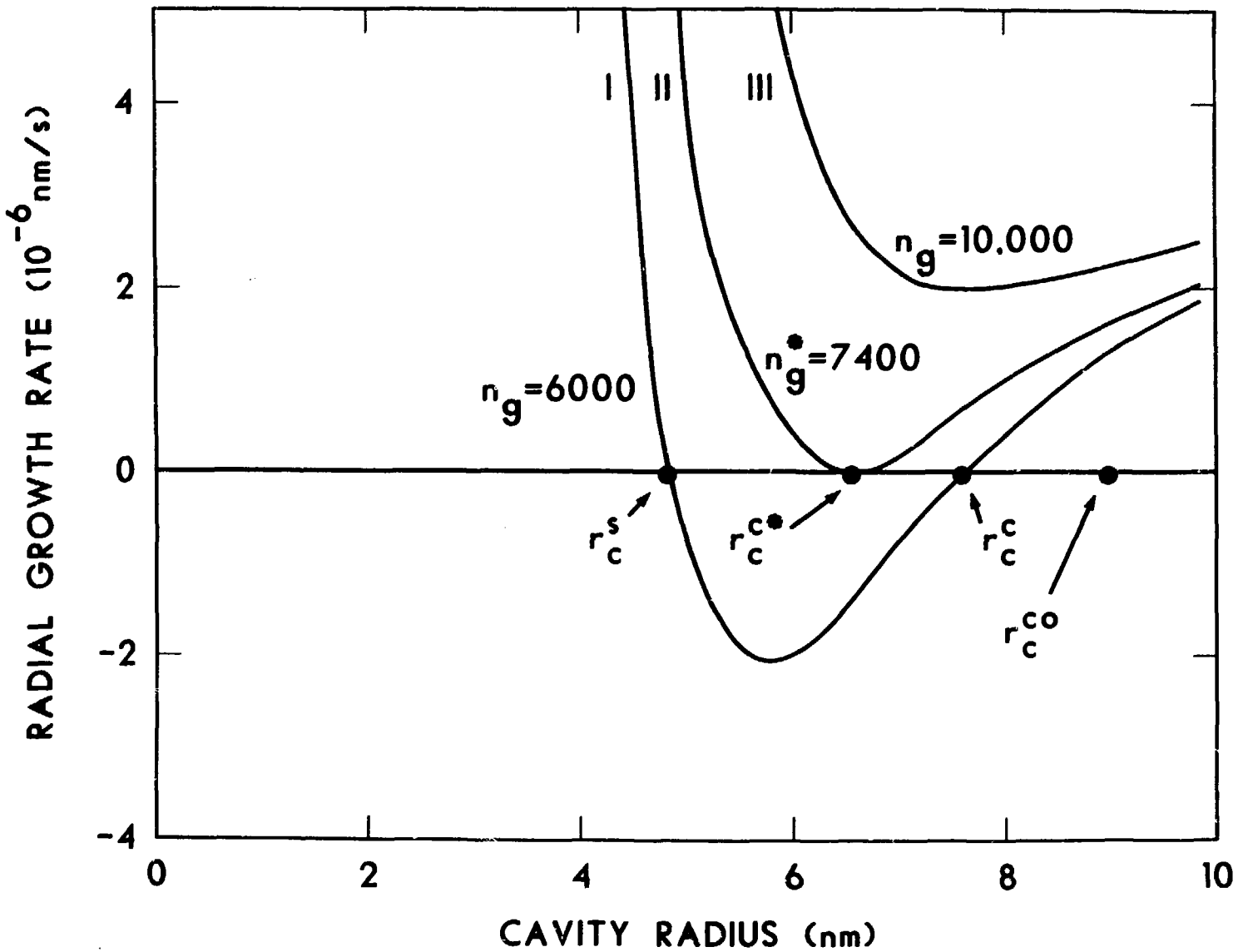

ORNL-DWG 83C-9336

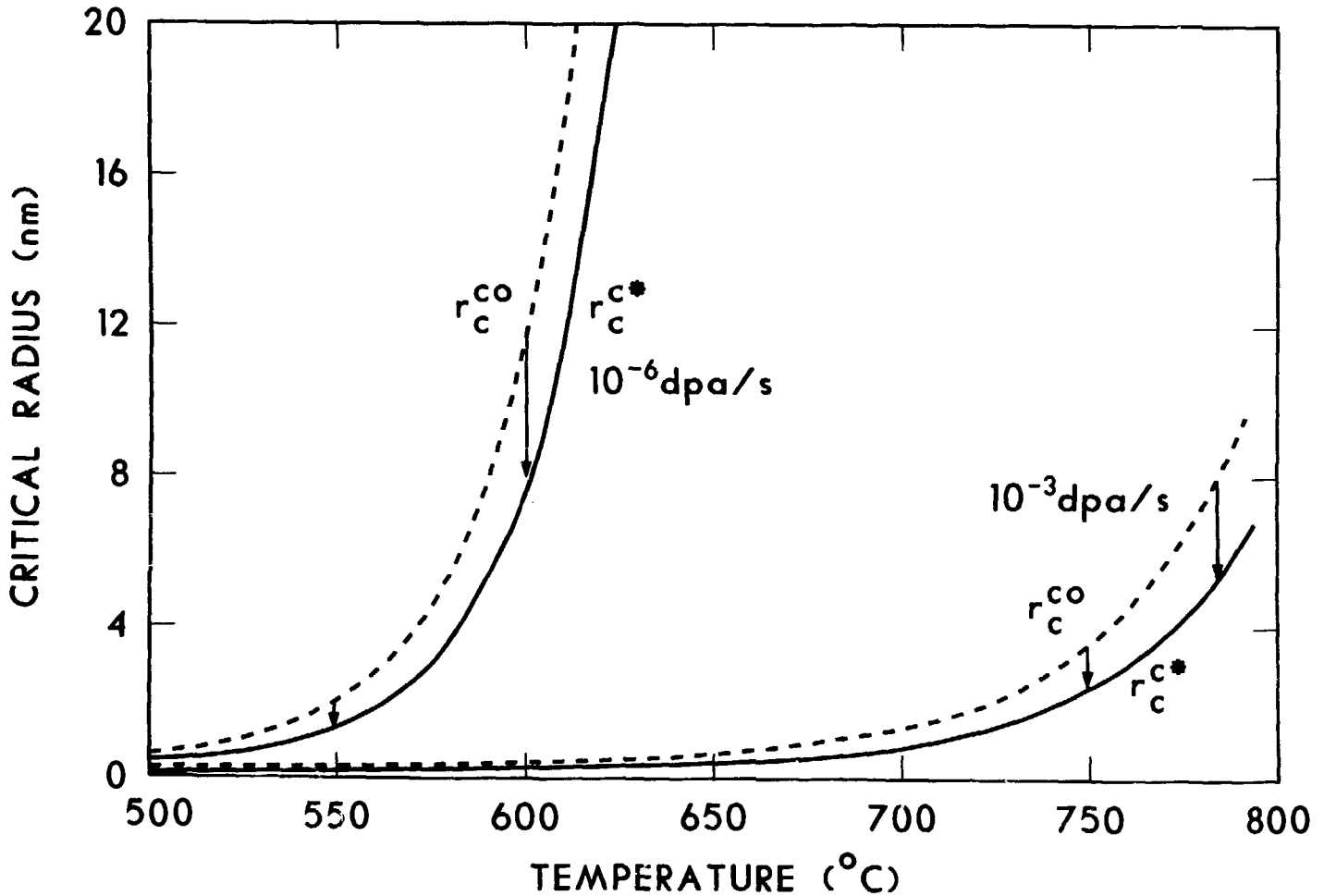

ORNL-DWG 83C-9346

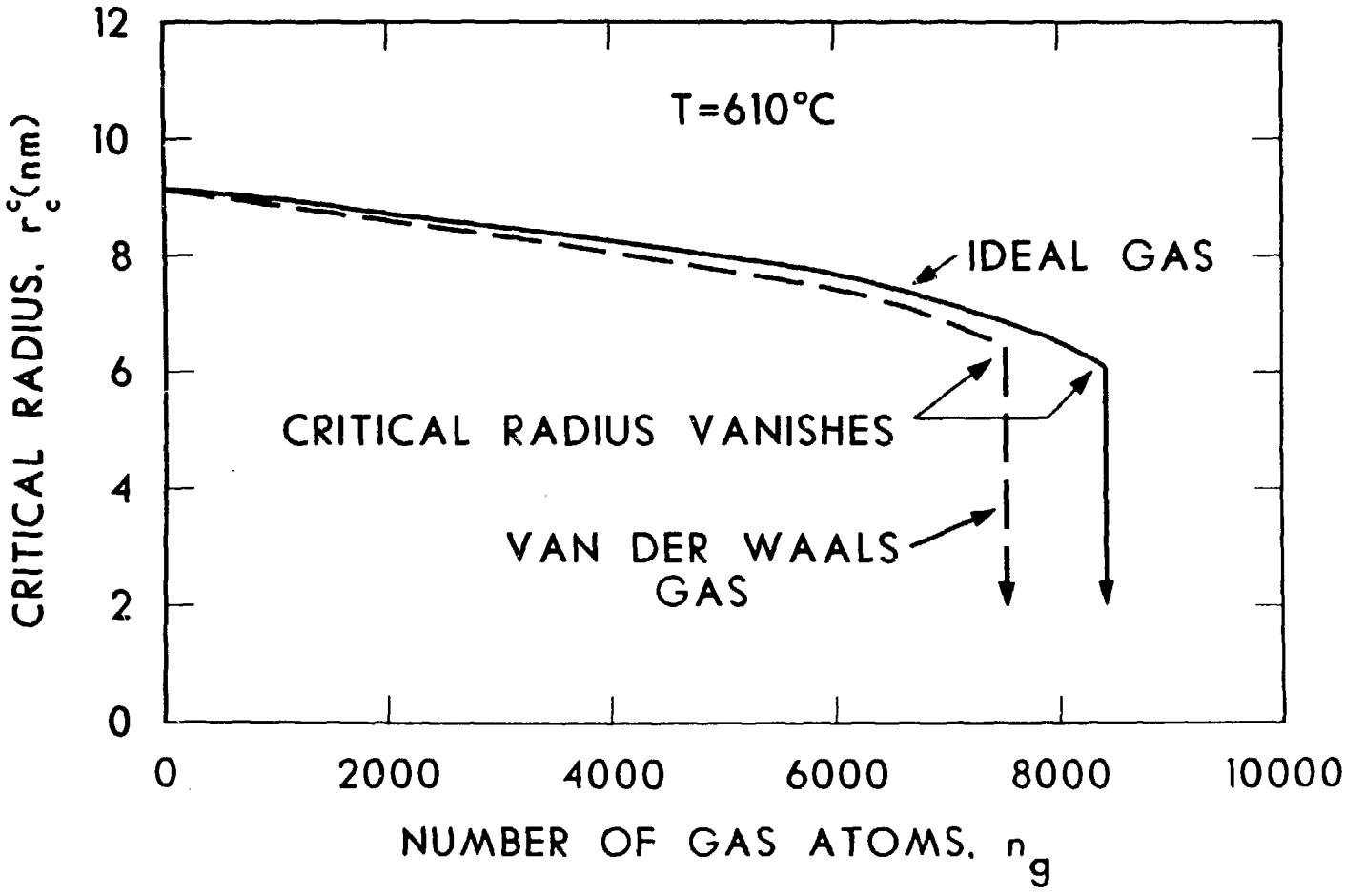

SIMPLE ANALYTICAL RESULTS HAVE BEEN DERIVED TO DESCRIBE THE CRITICAL RADIUS

$$r_c^{co} = \frac{2\gamma}{\frac{kT}{\Omega}\, n[(1 - Z)C_v/C_v^o + Z]}$$

$$r_c^{c*} = \frac{4\gamma}{\frac{3kT}{\Omega}\, n[(1 - Z)C_v/C_v^o + Z]}$$

$$n_g^* = \frac{128\pi\gamma^3\Omega^2}{81(kT)^3\{\, n[(1 - Z)C_v/C_v^o + Z]\}^2}$$

THE MINIMUM FINITE CRITICAL RADIUS IS RELATED TO THE GAS FREE CRITICAL RADIUS BY THE SIMPLE RESULT

$$\frac{r_c^{c*}}{r_c^{co}} = \frac{2}{3}$$

A SIMPLE ANALYTICAL RESULT DESCRIBES THE PRESSURE AT THE MINIMUM FINITE CRITICAL RADIUS

$$\frac{p_g(r_c^{c*})}{p_g^{eq}(r_c^{c*})} = \frac{1}{3}$$

WHEN ENOUGH GAS HAS BEEN ADDED TO THE CAVITY TO PRESSURIZE IT TO ONE-THIRD OR MORE OF ITS EQUILIBRIUM PRESSURE, AT THE SIZE r_c^{c*}, THE CRITICAL RADIUS VANISHES.

ANALYTICAL RESULTS HAVE ALSO BEEN OBTAINED FOR THE VAN DER WAALS GAS

$$r_c^{c*} = \frac{4\gamma}{3f}\left\{\frac{1}{2}\left(1 - \frac{2Bf}{kT - Bf}\right)\left(1 + \sqrt{1 + \eta}\right)\right\}$$

$$n_g^* = \frac{8\pi\gamma r_c^{c*2} - 16\pi f r_c^{c*3}/3}{kT - Bf}$$

WHERE

$$\eta = \frac{16B}{f(kT - Bf)} \Big/ \left(\frac{8B/3}{(kT - Bf)} - \frac{4}{3f}\right)^2$$

AND

$$f = \frac{kT}{\Omega}\,\ell n\,\left[(1 - Z)C_v/C_v^0 + Z\right]$$

RESULTS FOR THE VAN DER WAALS GAS ARE SIMILAR TO THOSE FOR THE IDEAL GAS EXCEPT AT VERY SMALL CAVITY SIZES.

ORNL-DWG 83-18876

THE VAN DER WAALS GAS LAW MAKES SOME IMPROVEMENTS IN THE CRITICAL QUANTITIES CALCULATED USING THE IDEAL GAS LAW

THE MINIMUM CRITICAL RADIUS IS CHANGED SOMEWHAT. FOR EXAMPLE, r_c^{c*}/r_c^{co} ~0.9 AT PRESSURES WHERE THE VAN DER WAALS LAW BREAKS DOWN. THE IDEAL GAS LAW GIVES $r^{c*}/r^{co} = 2/3$. SIMILARLY, P_g^*/P_g^{eq} ~0.15 FOR THE VAN DER WAALS AT THE HIGHEST PRESSURES, WHILE $P_g^*/P_g^{eq} = 1/3$ FOR THE IDEAL GAS.

THE CRITICAL NUMBER OF GAS ATOMS IS A STRONGER FUNCTION OF THE GAS LAW. THE VAN DER WAALS GAS LAW GIVES A SEVERAL-FOLD SMALLER n_g^* THAN THE IDEAL GAS AT THE HIGHEST PRESSURES.

IT IS IMPORTANT TO NOTE THAT THE IDEAL GAS ALWAYS GIVES A REASONABLY GOOD APPROXIMATION FOR CRITICAL RADIUS, AND GIVES A GOOD APPROXIMATION FOR CRITICAL NUMBER OF GAS ATOMS OVER WIDE RANGE OF CONDITIONS.

ORNL-DWG 83-18874

THE CRITICAL RADIUS CONCEPT IS USEFUL IN MAKING FURTHER PREDICTIONS ABOUT SWELLING

TEMPERATURE SHIFTS

BIMODAL CAVITY SIZE DISTRIBUTIONS

DIFFERENCES IN THE DOSE TO ONSET OF BIAS-DRIVEN SWELLING

- STRONG DEPENDENCE ON POINT DEFECT SINK STRENGTH
- STRONG DEPENDENCE ON GAS DILUTION AT INTERFACES

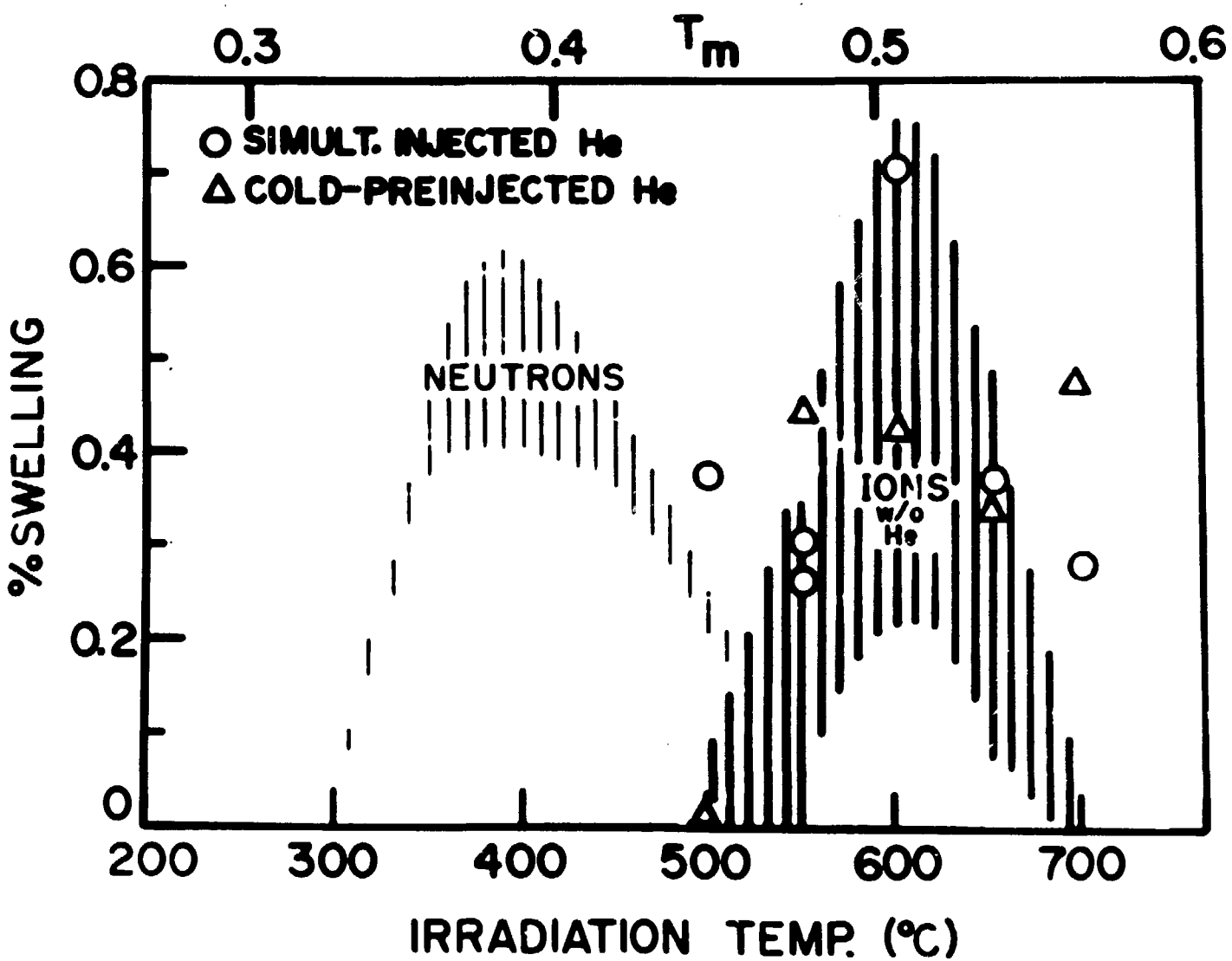
0.3
0.4
T_m
0.5
0.6
0.8
0.6
0.4
0.2
0
% SWELLING
O SIMULT. INJECTED He
Δ COLD-PREINJECTED He
NEUTRONS
IONS w/o He
200
300
400
500
600
700
IRRADIATION TEMP. (°C)

ORNL-DWG 78-21647

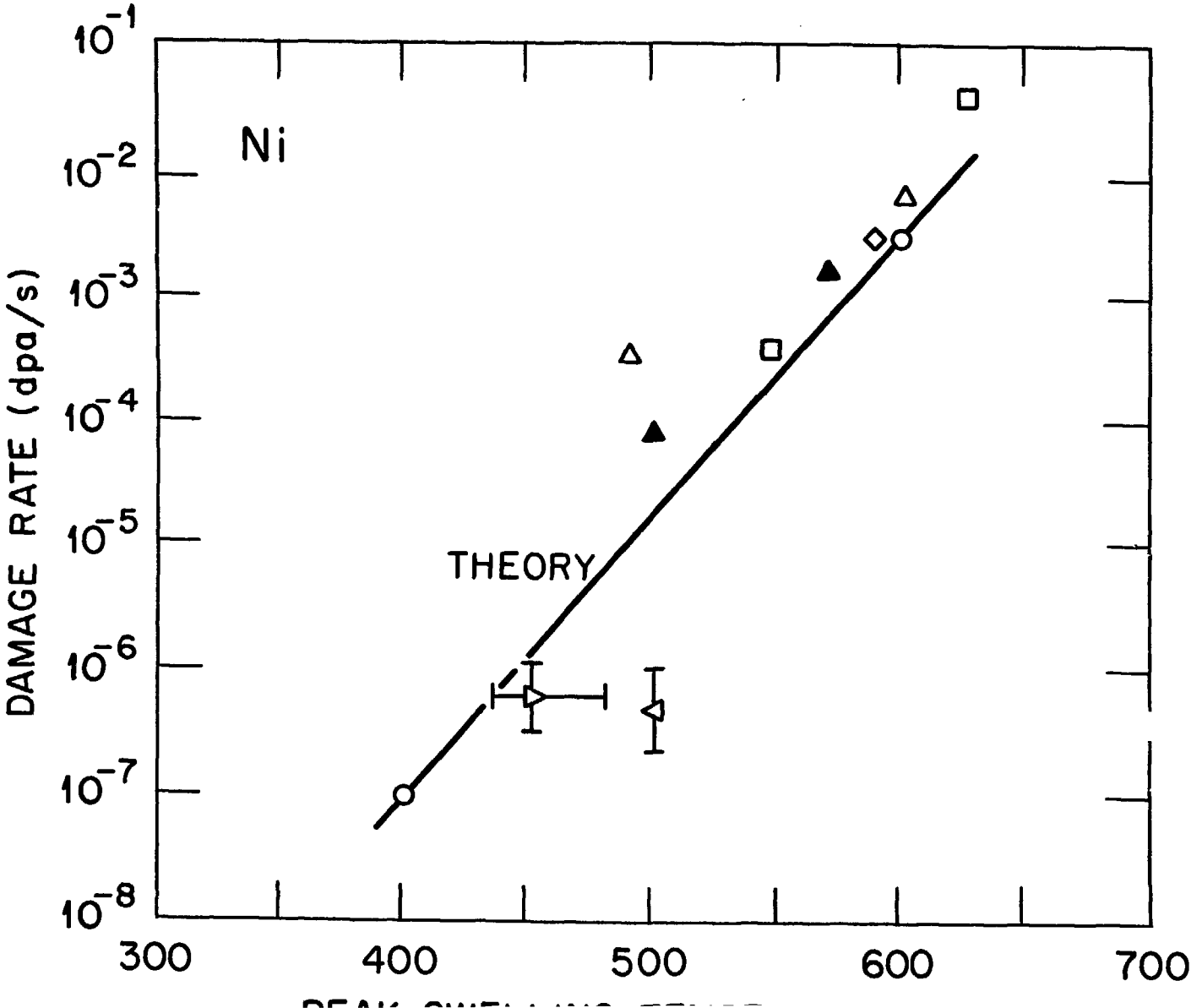

ORNL-DWG 83C-9349

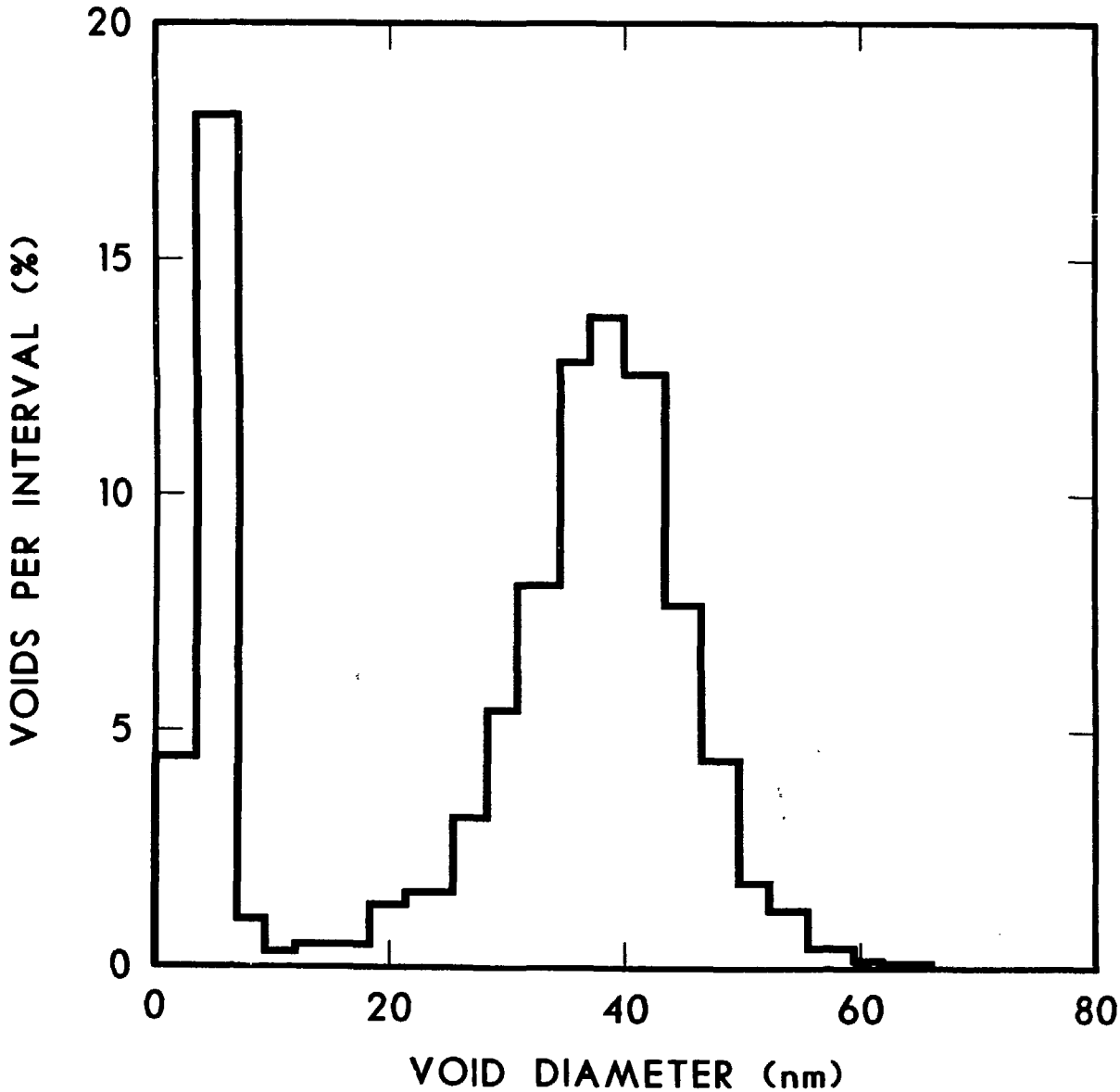

ORNL-DWG 83-18875

THE CRITICAL RADIUS AND CRITICAL NUMBER OF GAS ATOMS ARE STRONGLY DEPENDENT ON DISLOCATION SINK STRENGTH

IMPLICATIONS

WITHIN A GIVEN MATERIAL, CAVITY SWELLING WILL BE "PATCHY" ESPECIALLY EARLY IN DOSE, WHERE n_g^* HAS BEEN REACHED IN SOME REGIONS BUT NOT IN OTHERS.

THE TIME TO THE ONSET OF BIAS-DRIVEN SWELLING WILL VARY FOR TWO MATERIALS WITH DIFFERENT DISLOCATION DENSITIES.

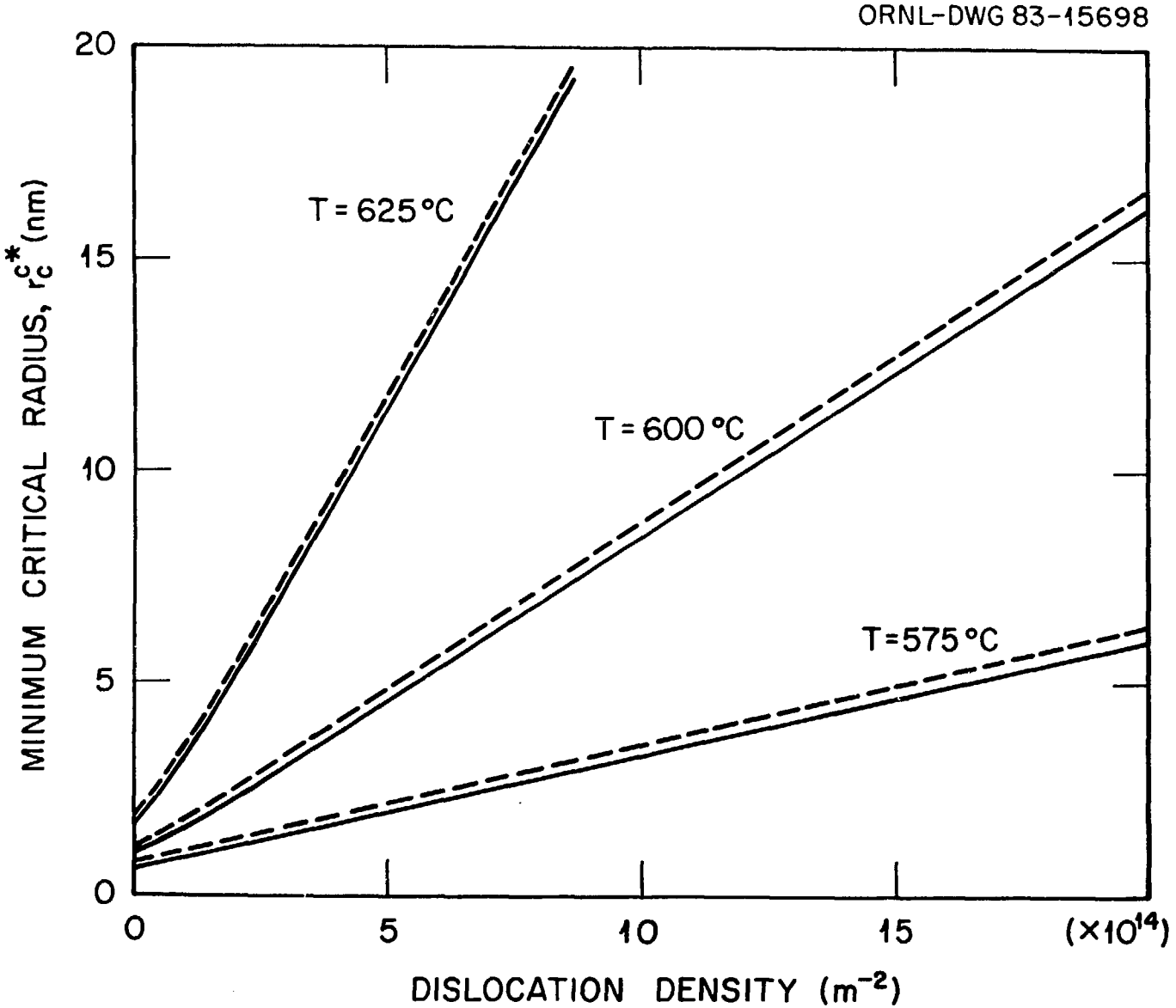
ORNL-DWG 83-15698
MINIMUM CRITICAL RADIUS, r_c^* (nm)
20
15
10
5
0
T = 625 °C
T = 600 °C
T = 575 °C
0
5
10
15
(×10^14)
DISLOCATION DENSITY (m^-2)

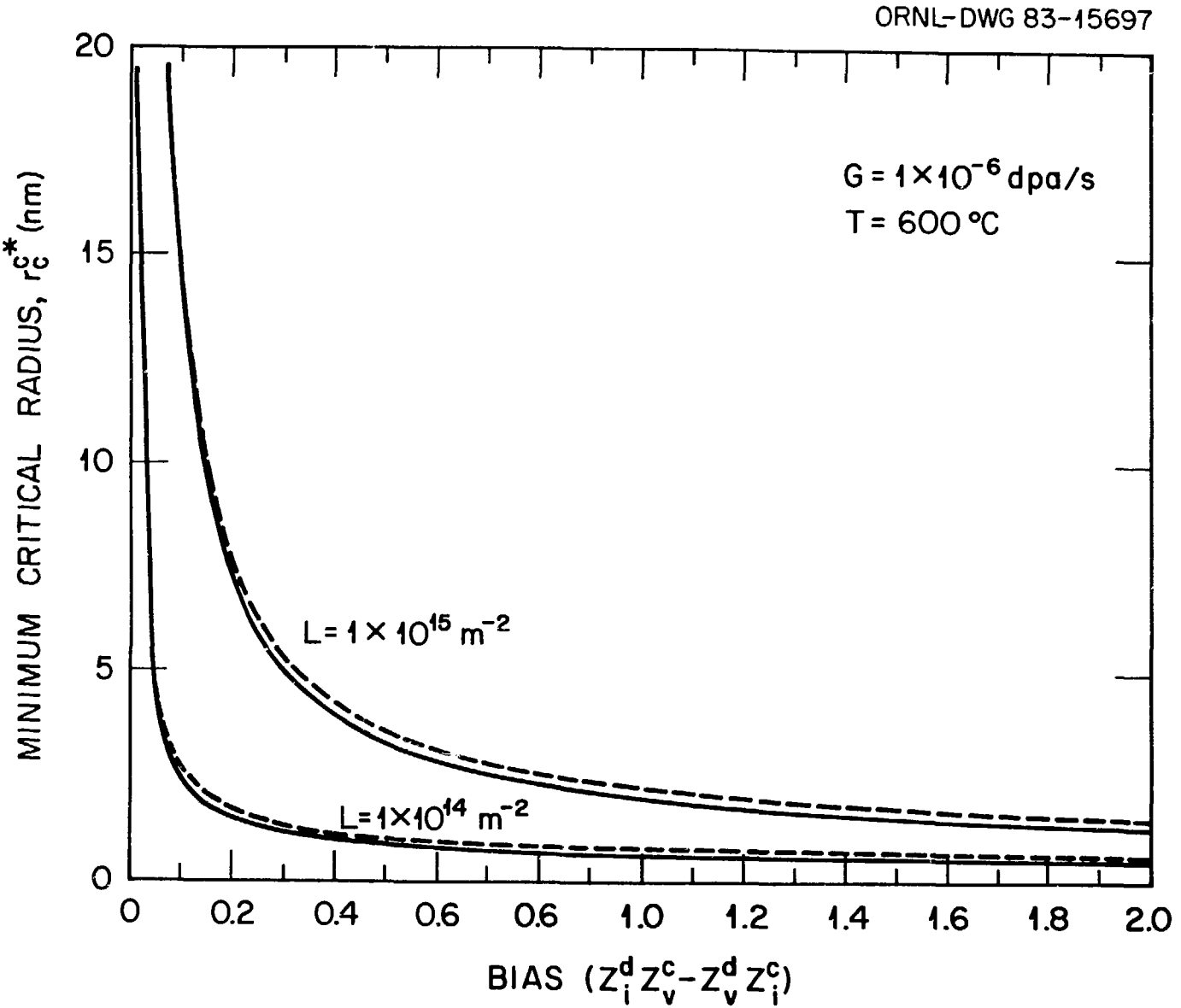
ORNL-DWG 83-15697
G = 1×10⁻⁶ dpa/s
T = 600 °C
L = 1 × 10¹⁵ m⁻²
L = 1×10¹⁴ m⁻²
MINIMUM CRITICAL RADIUS, r_c^{c*} (nm)
BIAS $(Z_i^d Z_v^c - Z_v^d Z_i^c)$
0
5
10
15
20
0
0.2
0.4
0.6
0.6
1.0
1.2
1.4
1.6
1.8
2.0

ORNL–DWG 82-9626

DOSE DEPENDENCE OF SWELLING IS DETERMINED BY THE RELATIVE RATES OF EVOLUTION OF THE VARIOUS MODES OF POINT DEFECT LOSS AND GENERATION

DOSE DEPENDENCE OF SWELLING CAN BE PREDICTED BY THE THEORY. FOR EXAMPLE, FOR RECOMBINATION MINOR AND DISLOCATION DENSITY SENSIBLY CONSTANT

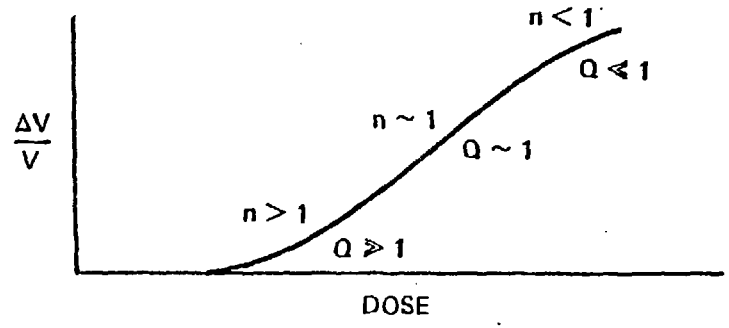

$$\frac{\Delta V}{V} \propto (\mathrm{DOSE})^n$$

$$Q = \frac{Z_v^d L}{4\pi r_c N_c Z_v^c}$$

[L. K. MANSUR, NUCLEAR TECHNOLOGY 40 (1978) 5–34]

EXPERIMENTALLY OBSERVED BEHAVIOR OF SEVERAL TYPES IS CONSISTENT WITH THIS PICTURE. KEY PARAMETER IS Q.

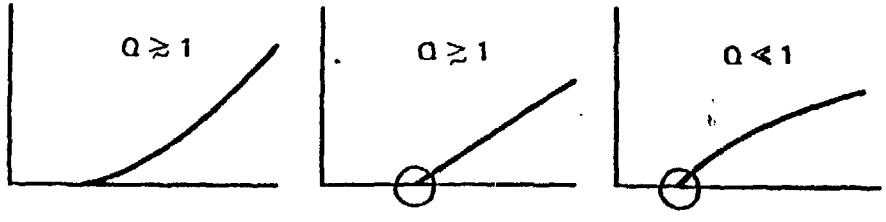

OBSERVED FOR FAST REACTOR IRRADIATION OF STAINLESS STEEL, LOW HELIUM, TYPICAL SINK STRENGTHS

OBSERVED FOR MATERIALS, WITH HIGH CAVITY DENSITY, HIGH HELIUM, LOW

MODE OF HELIUM INJECTION INFLUENCES EFFECT ON MICROSTRUCTURAL EVOLUTION

70 dpa, 625 C

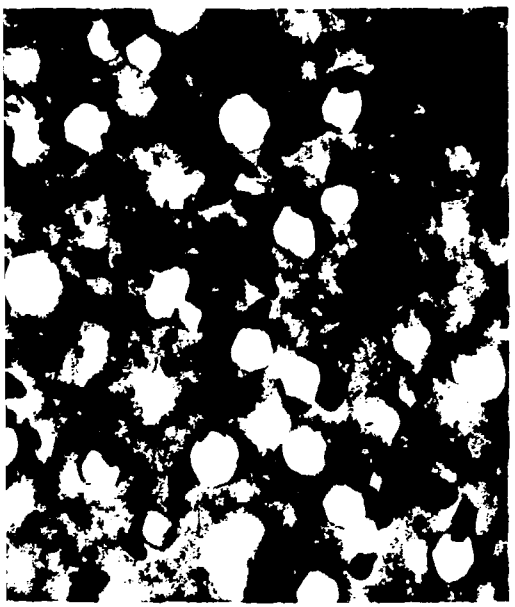

Simultaneous Helium
0.2 appm He/dpa

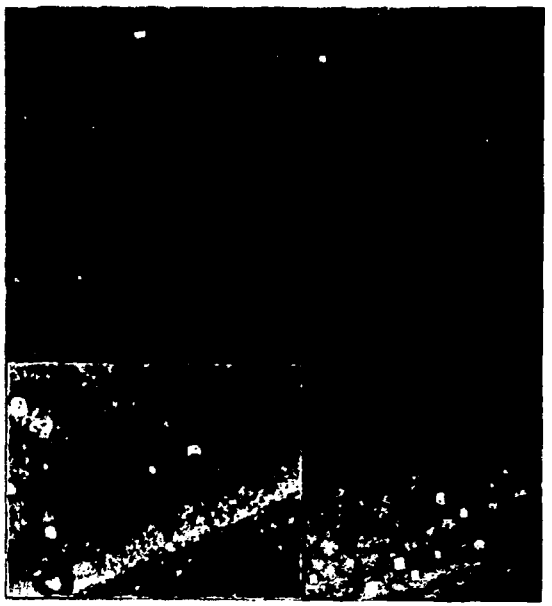

Preinjected Helium
14 appm He

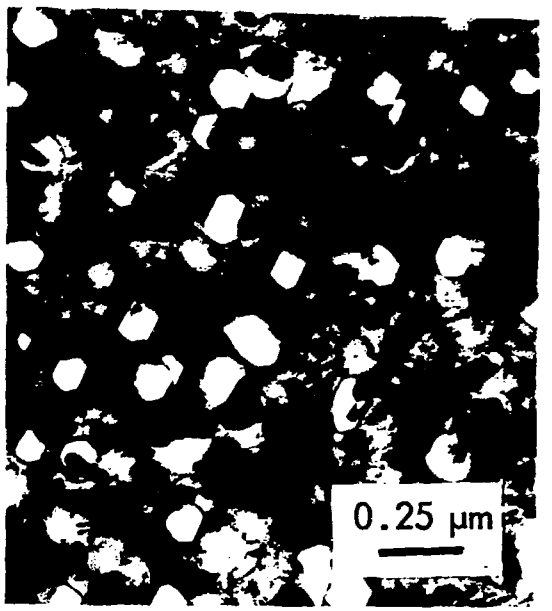

Injected At 10 dpa
14 appm He

- Swelling and Precipitation Behavior in Complex Phosphorous-Containing Austenitic Alloys — Critical Number of Gas Atoms and Alloy Design

ORNL-DWG 83-19018

HIGH PRECIPITATE-MATRIX INTERFACIAL AREA DELAYS THE ONSET OF BIAS DRIVEN SWELLING

AT HIGH TEMPERATURES OR LOW DOSE RATES, THE CRITICAL RADIUS FOR BIAS-DRIVEN GROWTH IS LARGE.

ADDING GAS REDUCES CRITICAL RADIUS. THERE IS A CRITICAL NUMBER OF GAS ATOMS IN A CAVITY, n_g^*, BEYOND WHICH THE CRITICAL RADIUS IS ZERO AND BIAS DRIVEN GROWTH IS CERTAIN.

A HIGH PRECIPITATE-MATRIX INTERFACIAL AREA INCREASES THE NUMBER OF CAVITIES AND THEREBY DECREASES THE NUMBER OF GAS ATOMS IN EACH CAVITY. AS A RESULT, THE TIME OF THE ACCUMULATION OF n_g^* GAS ATOMS IS INCREASED.

FINELY DISPERSED PRECIPITATES WITH HIGH INTERFACIAL AREA ARE THUS EXPECTED TO DELAY THE ONSET OF BIAS DRIVEN SWELLING.

WE BELIEVE THIS EFFECT HAS BEEN OBSERVED IN A PHOSPHIDE-PRECIPITATING AUSTENITIC STAINLESS STEEL.

ORNL-DWG 83-19014

BASE ALLOY COMPOSITION: B = (Fe-16Cr-14Ni+2.5Mo-2Mn-0.2Ti-0.04C)

ALLOY 1: B+(1.4Si-0.08P)

ALLOY 2: B+(0.7Si-0.04P)

THE PRINCIPAL EFFECT OF INCREASING THE P AND Si CONCENTRATION WAS TO INCREASE THE VOLUME FRACTION OF NEEDLE-SHAPED PHOSPHIDE PRECIPITATE DURING IRRADIATION.

THE ALLOYS WERE IRRADIATED TO A DOSE OF ~32 dpa (E > 0.1 MeV) IN EBR-II AT 555°C. IN ALLOY 1 WHERE THE P AND Si CONCENTRTIONS ARE TWICE AS HIGH AS IN ALLOY 2, THE PRECIPITATE NUMBER DENSITY IS THREE TIMES AS HIGH. THE AVERAGE SIZE OF THE PRECIPITATES ALSO INCREASED BY A FACTOR OF 1.5 ~ 2. AS A RESULT THE PRECIPITATE-MATRIX INTERFACIAL AREA IS NINE TIMES AS LARGE IN ALLOY 1. IN ALLOY 1, SWELLING WAS TOTALLY SUPPRESSED.

ORNL-PHOTO 3217-83

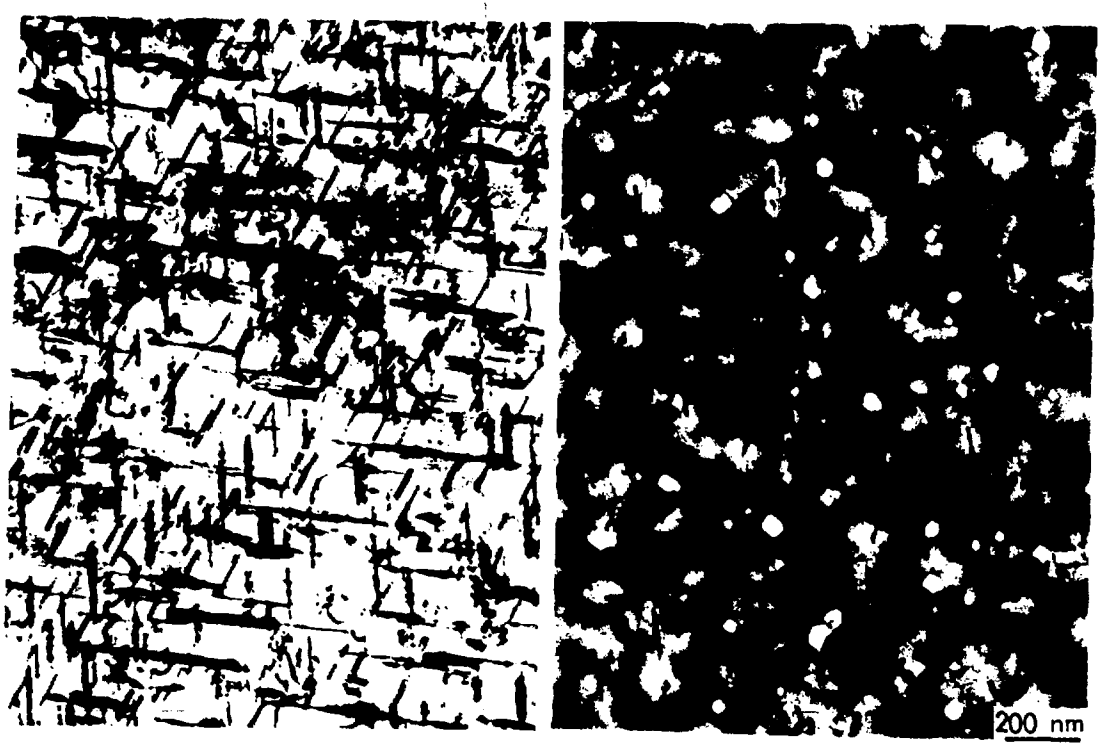

ORNL-DWG 83-19016

Alloy	Dose (dpa)	Dislocation density (m^{-2})	Average cavity diameter (nm)	Cavity density (m^{-3})	Average ppt. dimension (nm)	Precipitate density (m^{-3})	He-atoms per bubble, n_g (m^{-3})	Calculated n_g^*
1	32	8×10^{13}	--	$\sim 1.8 \times 10^{21}$	300×20×10	6×10^{20}	730	1210
2	32	3.1×10^{14}	35	$\sim 2.0 \times 10^{20}$	200×10×5	2×10^{20}	6500	3750

NO SWELLING WAS OBSERVED IN ALLOY 1, WHILE SWELLING WAS OBSERVED IN ALLOY 2. THIS CORRELATES WELL WITH THE FACT THAT n_g^* CALCULATED FOR ALLOY 1 IS LARGER THAN THE MAXIMUM POSSIBLE NUMBER OF GAS ATOMS IN A CAVITY, WHILE n_g^* CALCULATED FOR ALLOY 2 IS LESS THAN THE MAXIMUM NUMBER OF GAS ATOMS IN A CAVITY.

ION IRRADIATION AT 675°C ON ALLOY 1 TO 90 dpa WITH 0.4 appm/dpa ALSO REVEALS A VERY HIGH DENSITY OF CAVITIES ON PHOSPHIDE-MATRIX INTERFACES AND AGAIN SHOWS NO SWELLING.

ORNL-DWG 83-19019

CONCLUSIONS

INCREASING THE VOLUME FRACTION OF NEEDLE-SHAPED IRON PHOSPHIDE PHASE IN AUSTENITIC STAINLESS STEELS INHIBITS VOID SWELLING. THE ANALYSIS INDICATES THAT HELIUM DISPERSION BY THE FORMATION OF MANY SMALL CAVITIES EXTENDS THE TIME TO THE ACCUMULATION OF THE CRITICAL NUMBER OF GAS ATOMS IN EACH CAVITY.

THE RESULT SUGGESTS THAT THE INTRODUCTION OF A HIGH DENSITY OF STABLE PRECIPITATE PARTICLES DURING IRRADIATION MAY OFFER THE POSSIBILITY OF SIGNIFICANTLY DELAYING THE ONSET OF BIAS-DRIVEN SWELLING.

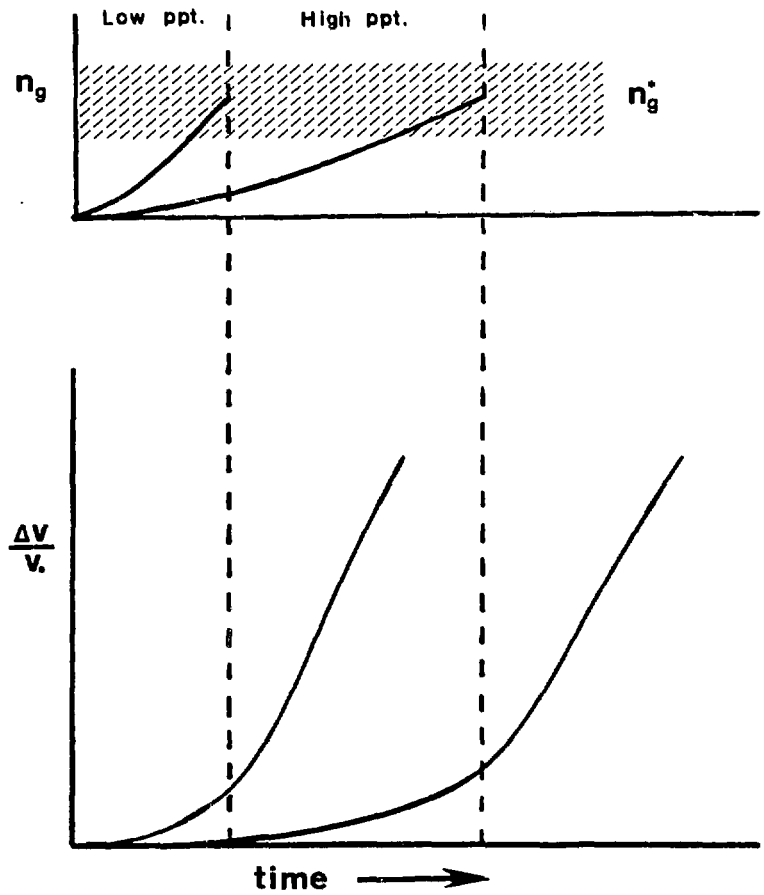

- The Effects of Helium and Its Mode of Introduction on the Microstructural Response of a Stable Austenitic Alloy

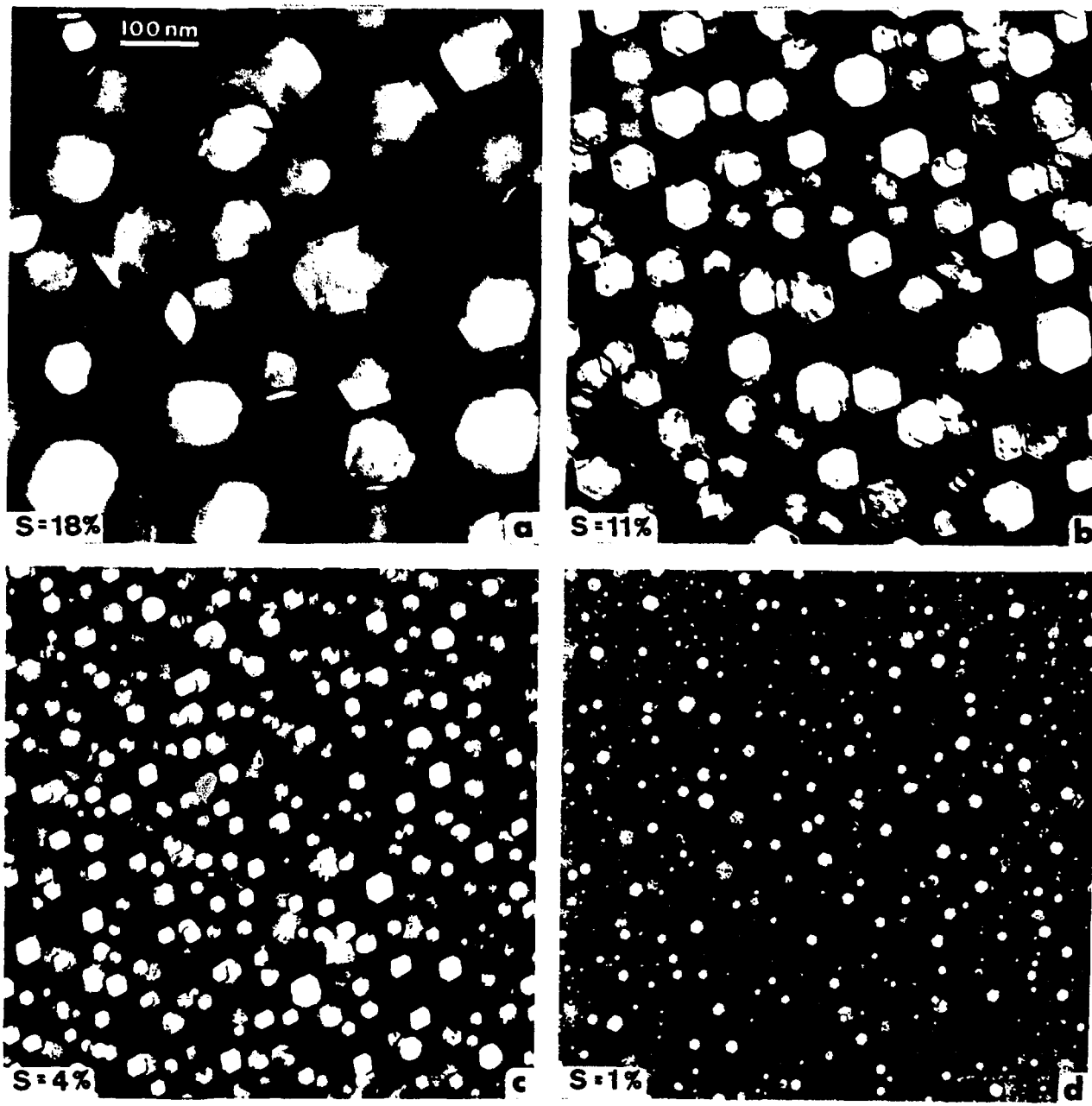
100 nm
S=18%
a
S=11%
b
S=4%
c
S=1%
d

ORNL-DWG 82-12540

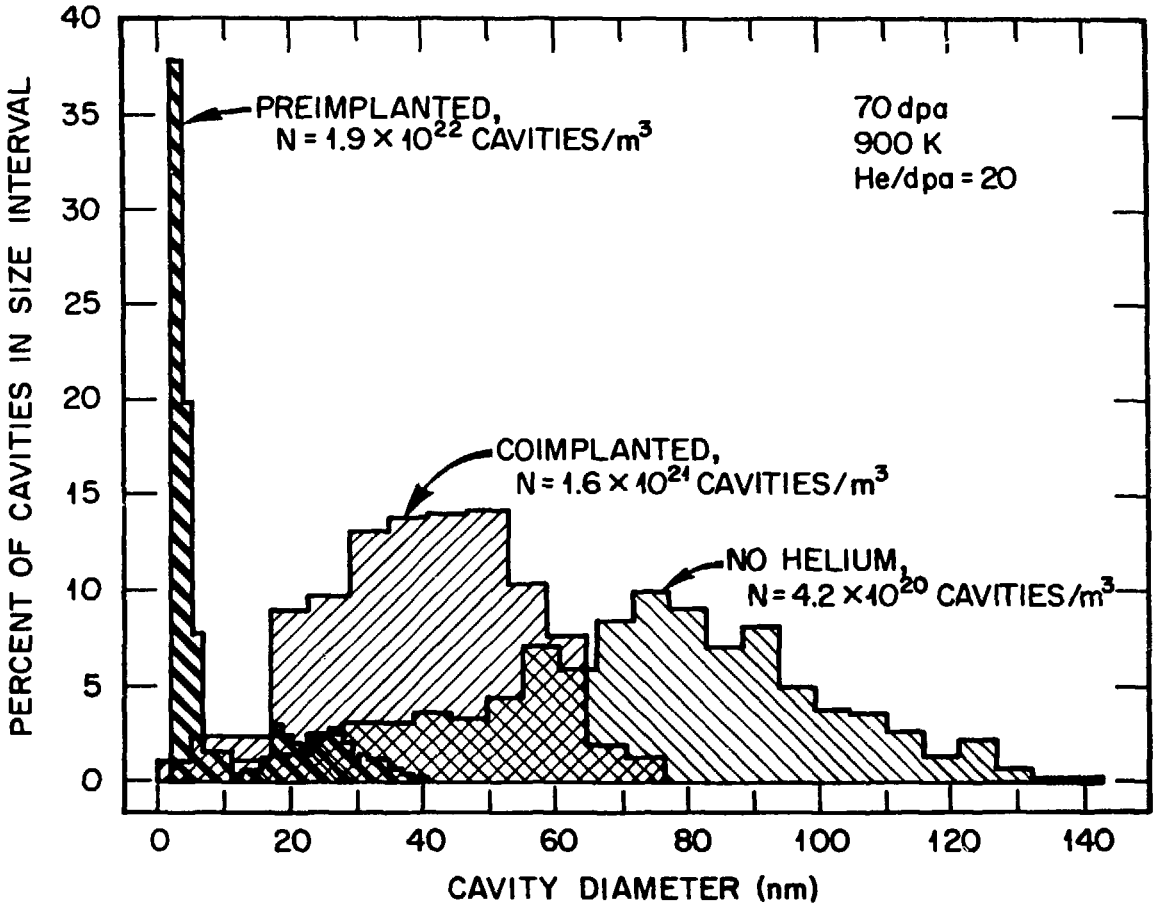

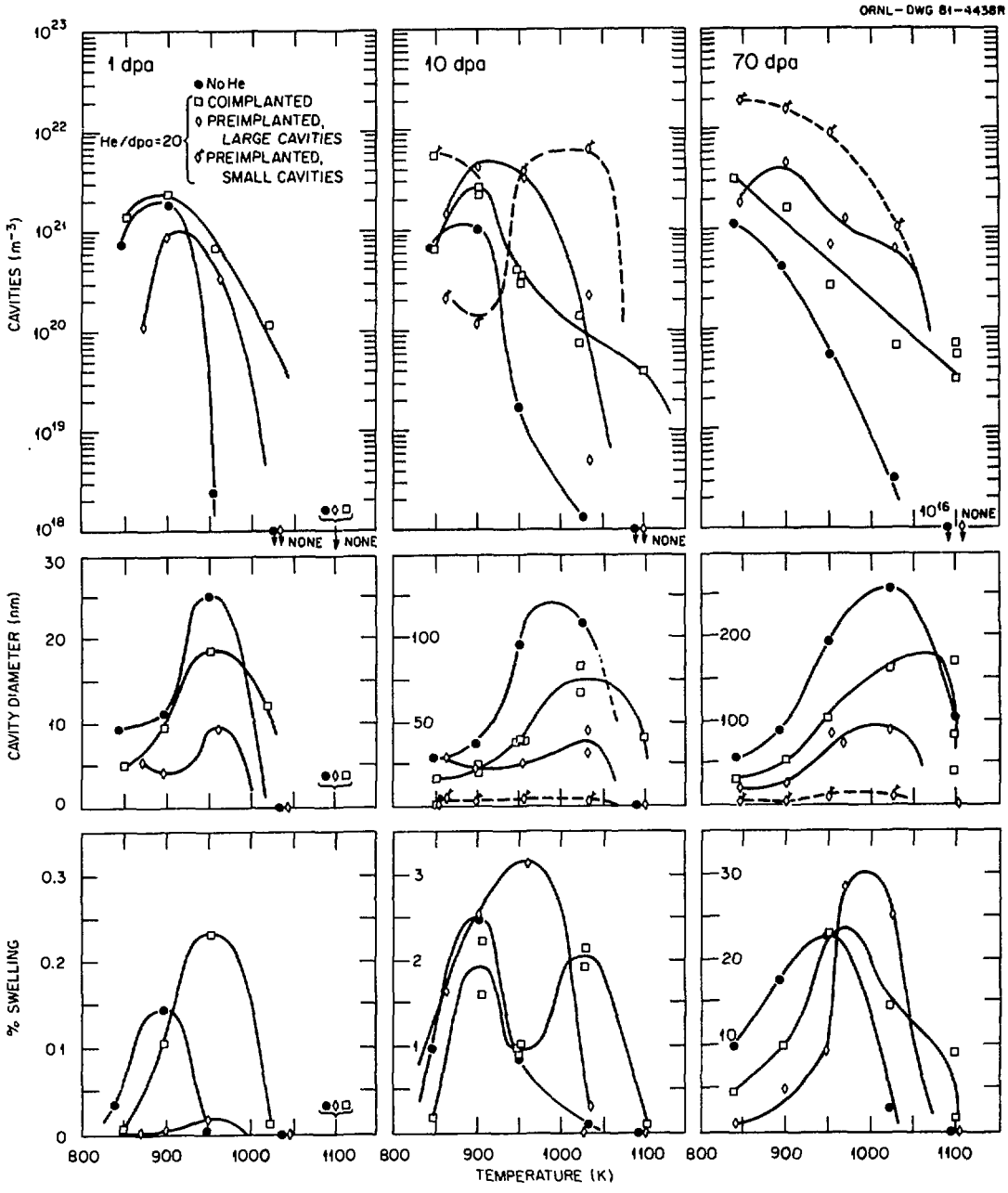
ORNL-DWG 81-4438R
1 dpa
10 dpa
70 dpa
● No He
□ COIMPLANTED
◊ PREIMPLANTED, LARGE CAVITIES
♂ PREIMPLANTED, SMALL CAVITIES
He/dpa=20
CAVITIES (m⁻³)
CAVITY DIAMETER (nm)
% SWELLING
NONE
TEMPERATURE (K)

ORNL-DWG 81-18112R

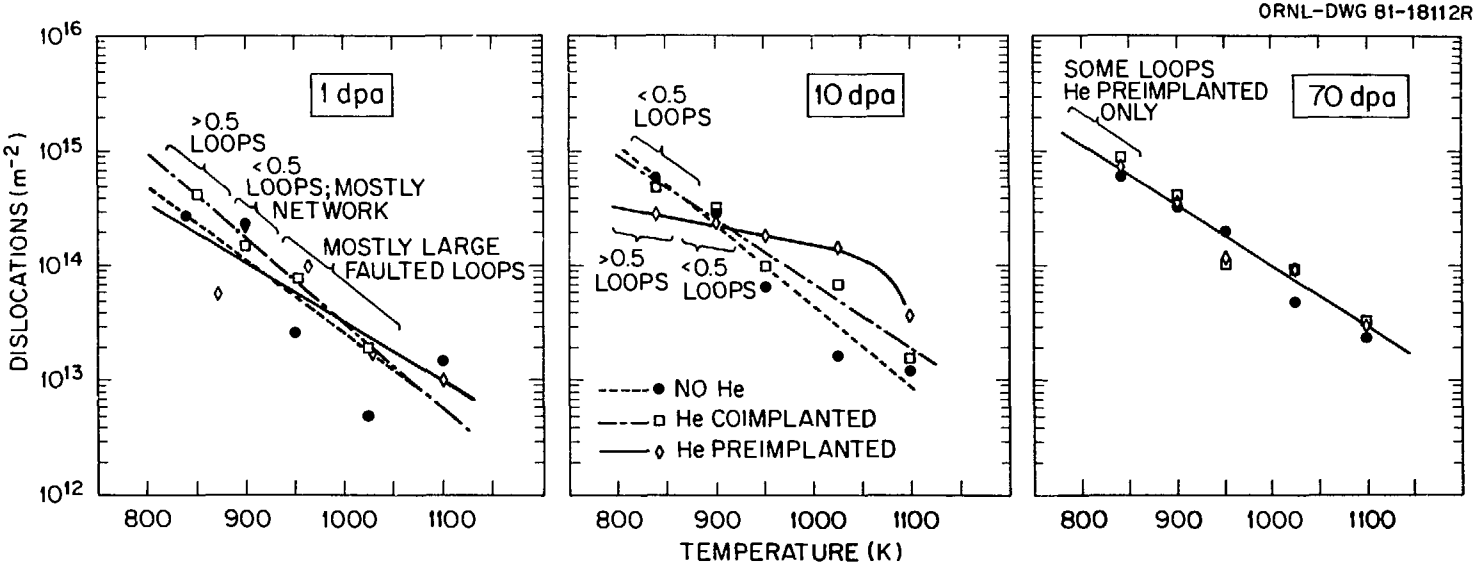

ORNL-DWG 83-19022

CONCLUSIONS

PREINJECTION AT ROOM TEMPERATURE IS A POOR TECHNIQUE TO SIMULATE SIMULTANEOUS INJECTION SWELLING RESULTS. PREINJECTION AT THE BOMBARDMENT TEMPERATURE IS BETTER.

THE METHOD OF INTRODUCING HELIUM IN A SIMULATION EXPERIMENT CAN CONSIDERABLY INFLUENCE THE FINAL DAMAGE MORPHOLOGY.

WITHOUT ADDED GAS, BOMBARDMENT WITH 4 MeV Ni IONS TO A DAMAGE LEVEL OF 70 dpa AT 625°C PRODUCED A SWELLING OF 18.1%.

SIMULTANEOUS INJECTION OF HELIUM AT A RATE OF 20 appm PER dpa OF DAMAGE (A FUSION REACTOR ENVIRONMENT) GAVE RISE TO LESSER (10.9%) SWELLING. PREINJECTING THE SAME TOTAL AMOUNT OF He (1400 appm), AN EXPERIMENTALLY SIMPLER TECHNIQUE, RESULTED IN A MUCH GREATER SUPPRESSION OF SWELLING THROUGH INTENSIFIED CAVITY NUCLEATION.

PREINJECTION AT 625°C FOLLOWED DIRECTLY BY HEAVY ION BOMBARDMENT AT THE SAME TEMPERATURE YIELDED A SWELLING OF 3.7%, WHILE PREINJECTION AT ROOM TEMPERATURE PRODUCED THE MOST PROFUSE CAVITY NUCLEATION AND A SWELLING OF ONLY 1.1%.

- Through-Range Ion Damage in Nickel

ORNL-DWG. 81-17596

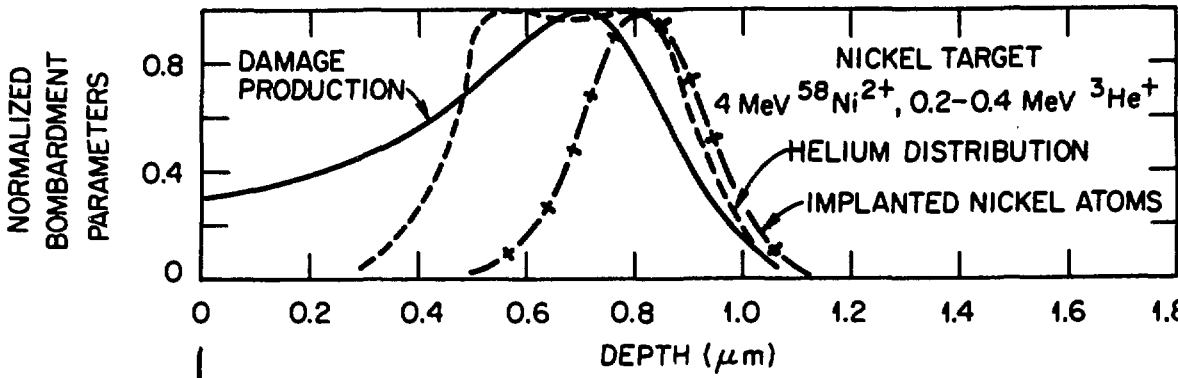

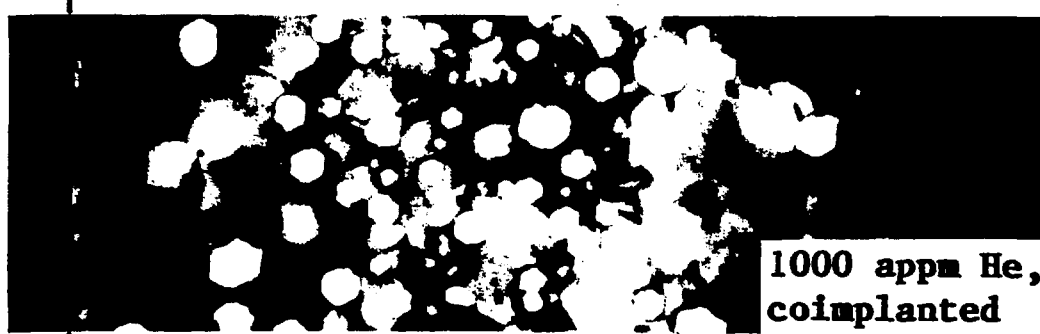

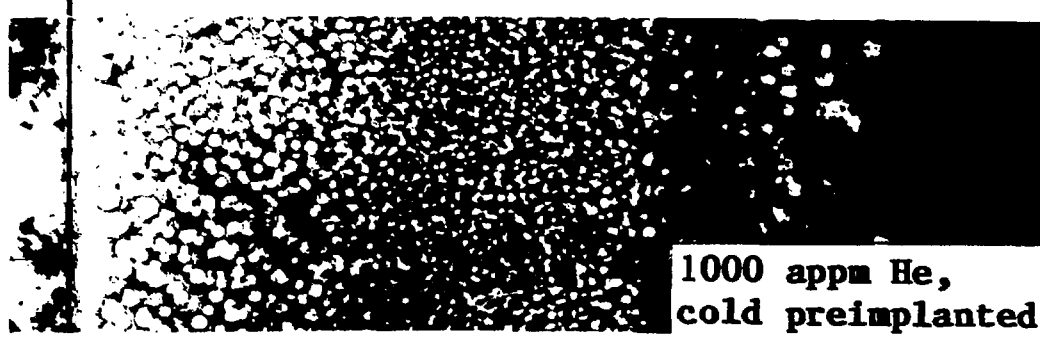

Nickel, implanted with helium and bombarded with nickel ions, 873 K and 50 dpa peak damage.

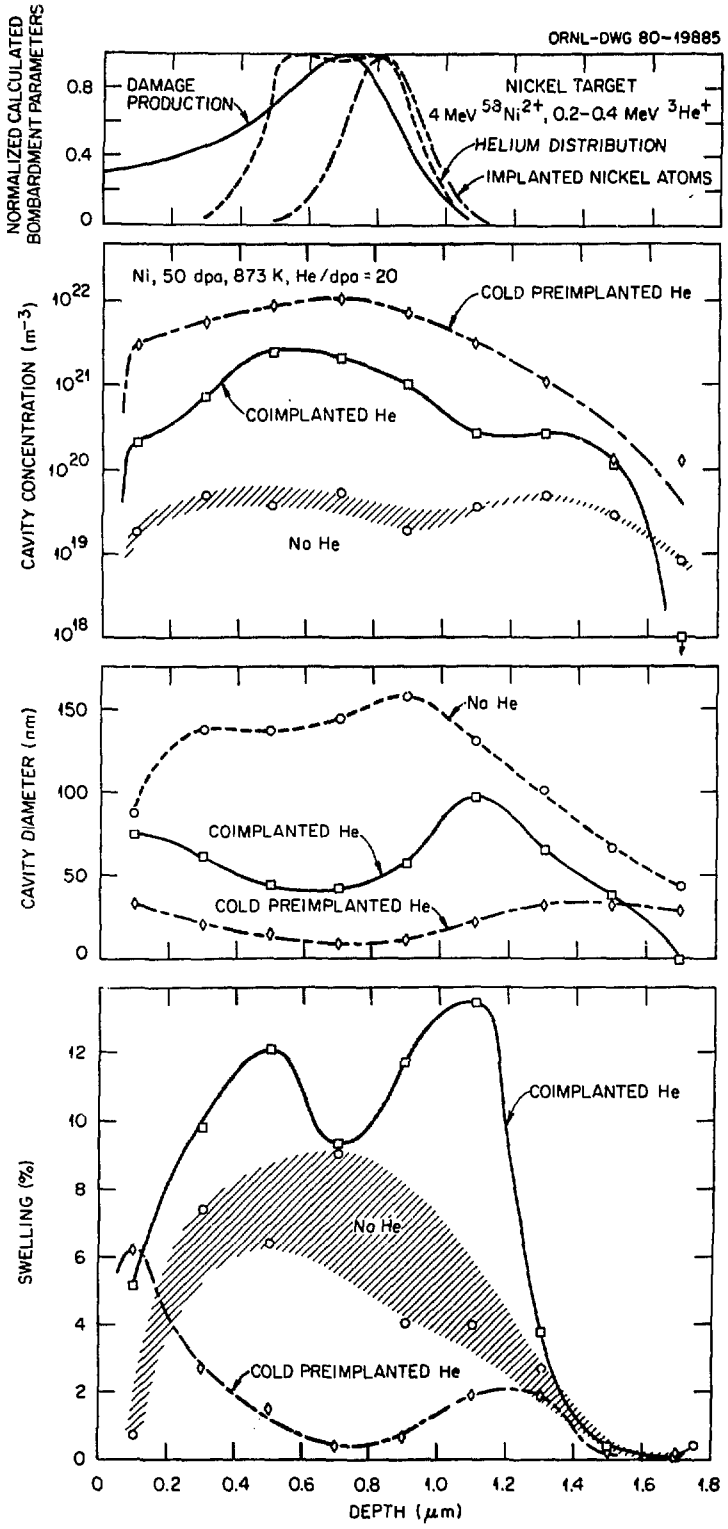
ORNL-DWG 80-19885
NORMALIZED CALCULATED BOMBARDMENT PARAMETERS
DAMAGE PRODUCTION
NICKEL TARGET
4 MeV $^{58}Ni^{2+}$, 0.2-0.4 MeV $^{3}He^{+}$
HELIUM DISTRIBUTION
IMPLANTED NICKEL ATOMS
Ni, 50 dpa, 873 K, He/dpa = 20
CAVITY CONCENTRATION (m^{-3})
COLD PREIMPLANTED He
COIMPLANTED He
No He
CAVITY DIAMETER (nm)
SWELLING (%)
DEPTH (μm)

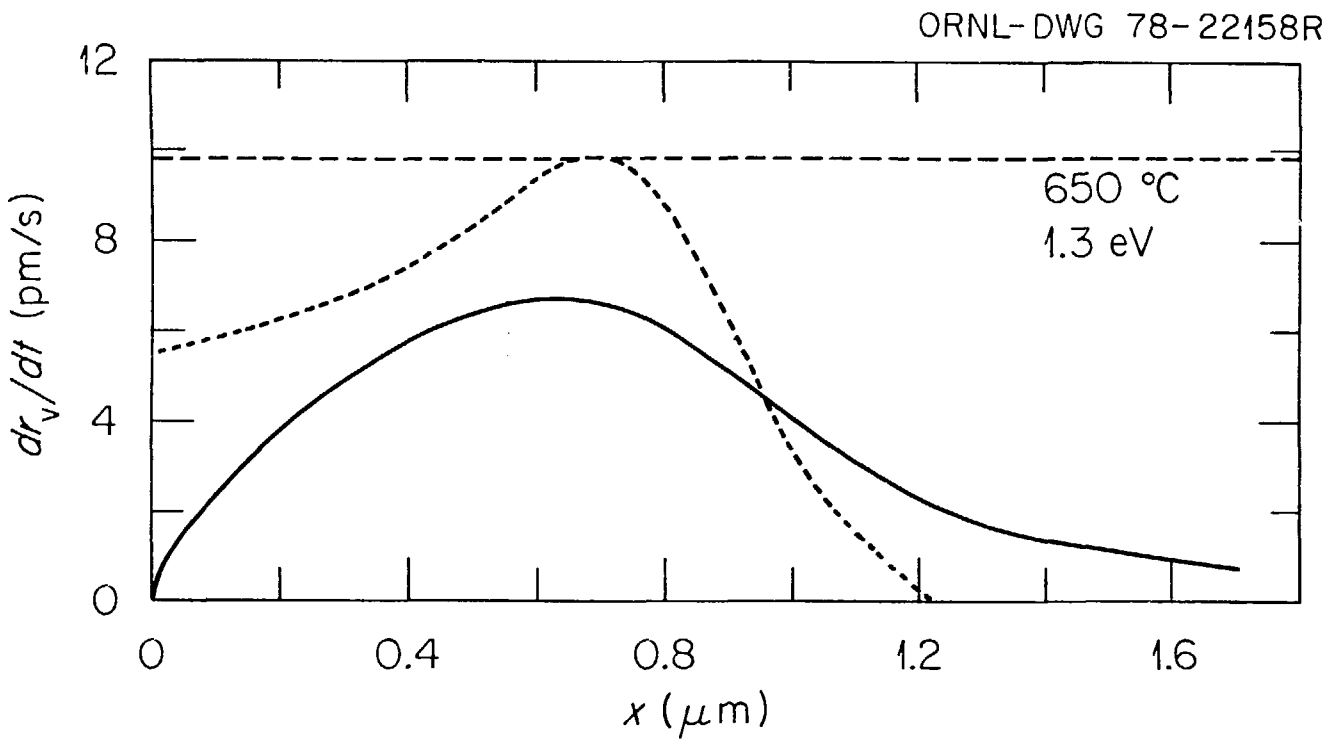
ORNL-DWG 78-22158R
12
8
4
0
dr_v/dt (pm/s)
650 °C
1.3 eV
0
0.4
0.8
1.2
1.6
x (μm)

ORNL-DWG 83-19020

MAJOR OBSERVATIONS IN THROUGH-RANGE MICROSTRUCTURE EXPERIMENT

HELIUM REFINES THE CAVITY DISTRIBUTION AND LEADS TO LOWERING OF SWELLING

SWELLING AND MICROSTRUCTURE ARE DEPLETED NEAR THE SURFACE

SWELLING PENETRATES SIGNIFICANTLY DEEPER THAN THE POINT DEFECT PRODUCTION PROFILE

OBSERVATIONS ARE IN GOOD AGREEMENT WITH THEORETICAL PREDICTIONS

CAVITIES BECOME THE DOMINANT SINK, LEADING TO LOWERING OF SWELLING RATE

POINT DEFECT ANNIHILATION AT THE SURFACE LOWERS POINT DEFECT CONCENTRATIONS NEAR THE SURFACE AND INHIBITS SWELLING

DIFFUSIONAL SPREADING OF POINT DEFECTS BEYOND THE DAMAGE DEPTH

- Neutron Irradiation Studies of Iron and Vanadium

ORNL-DWG 83-18625

EXPERIMENTAL PROCEDURES

MATERIALS:

Fe: 2-PASS ZONE REFINED, 50 wppm INTERSTITIAL IMPURITIES (2 appm ^{10}B)

V: 2-PASS ZONE REFINED, 100 wppm INTERSTITIAL IMPURITIES

V-B_4C: V WITH BORON CARBIDE ADDITIONS (3900 appm ^{10}B)

IRRADIATION:

- SEALED IN CAPSULES IN OAK RIDGE RESEARCH REACTOR
- TEMPERATURES

  Fe: 182–500°C (0.25 to 0.42 T_m)

  V: 182–500°C (0.21 to 0.36 T_m)

  V-B_4C: 450–650°C

FLUENCE:

~1 dpa (~1 × 10^{25} n/m^2, E > 0.1 MeV)

HELIUM: FROM BORON, $^{10}B(n,\alpha)\,^{7}Li$ REACTION

Fe: 2 appm/dpa (HALOS) (<0.1 appm/dpa FROM MATRIX)

V: <0.1 appm/dpa

V-B_4C: 3900 appm/dpa (HOMOGENEOUSLY DISTRIBUTED)

ORNL-DWG 83-19008

DISLOCATION MICROSTRUCTURES: Fe, V

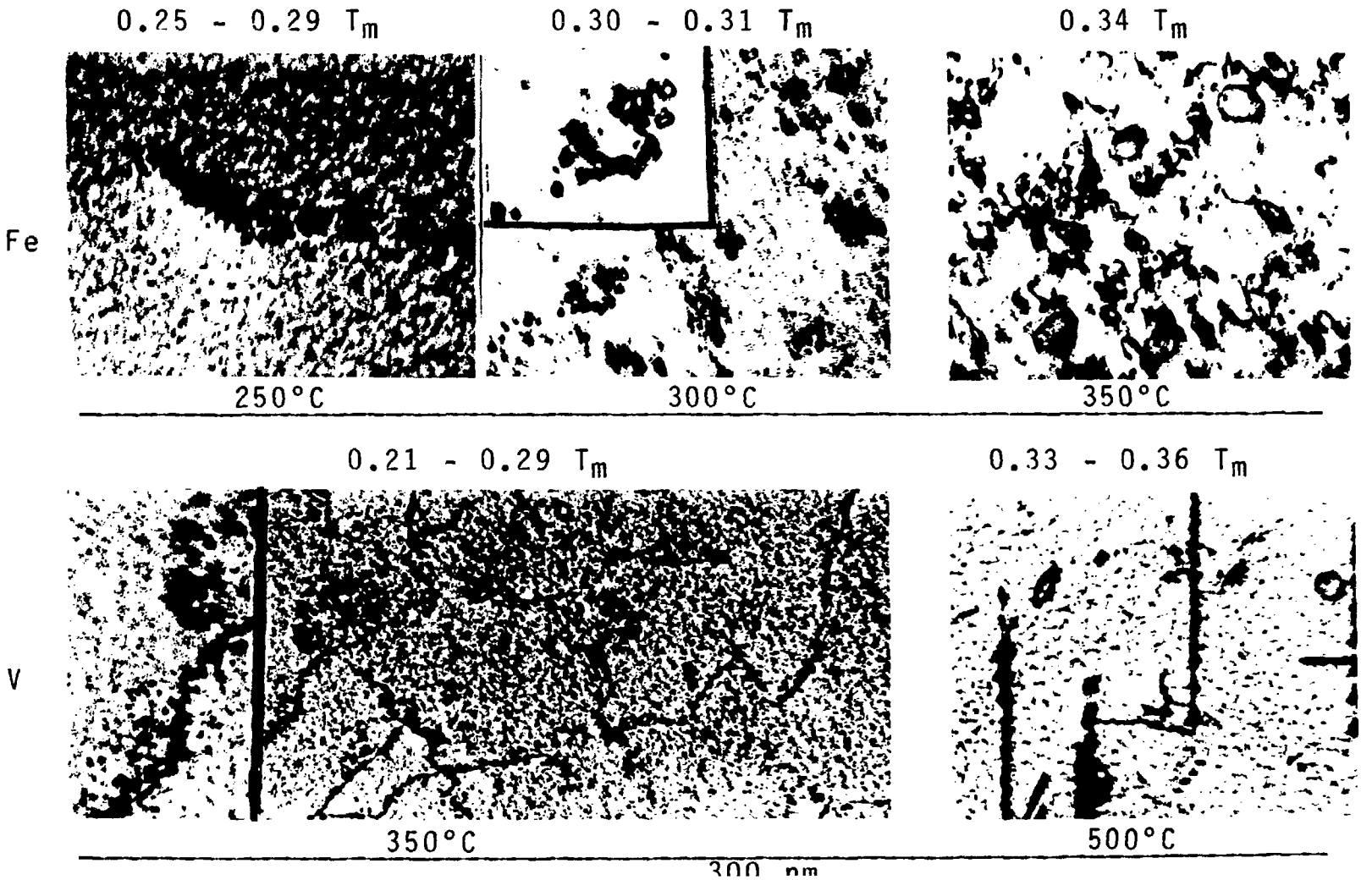

ORNL-DWG 83-18626

COMPARISON OF DISLOCATION MICROSTRUCTURES: V, Fe

- IN Fe, THE DISLOCATION MICROSTRUCTURES WERE:
  - 0.25–0.29 T_m DECORATED DISLOCATION LINE SEGMENTS
  - 0.30–0.31 T_m CLUSTERS OF LOOPS
  - 0.34 T_m HOMOGENEOUSLY DISTRIBUTED LOOPS
  - 0.37–0.42 T_m COARSE DISTRIBUTION OF LOOPS WITH LINE SEGMENTS
- IN V, THE DISLOCATION MICROSTRUCTURES WERE:
  - 0.21–0.29 T_m CLUSTERS OF LOOPS AT LINE SEGMENTS
  - 0.33–0.36 T_m COARSE, HOMOGENEOUS DISTRIBUTION OF LOOPS AND SOME LINE SEGMENTS
- IN BOTH V AND Fe, LOOPS WITHIN LOOP CLUSTERS DO NOT HAVE THE SAME SPECIFIC BURGERS VECTOR.
- BURGERS VECTORS OF DISLOCATION LOOPS ARE PREDOMINANTLY a<100> IN Fe AND ARE a/2<111> IN V.

HELIUM EFFECTS: DISLOCATIONS

Fe:

- FOR IRRADIATION TEMPERATURES OF 220–450°C, HALOS CONSIST OF DISLOCATION LOOPS. THE LOOPS IN BOTH THE HALO AND NONHALO REGIONS ARE INTERSTITIAL WITH $\underline{b}$ = a<100>.
- IN THE HALOS, THE LOOP CONCENTRATION IS HIGHER AND THE LOOP DIAMETER SMALLER THAN IN NONHALO REGIONS. AT 450°C, THE DISLOCATION DENSITY IS AN ORDER OF MAGNITUDE HIGHER IN THE HELIUM HALO THAN IN NONHALO REGIONS.

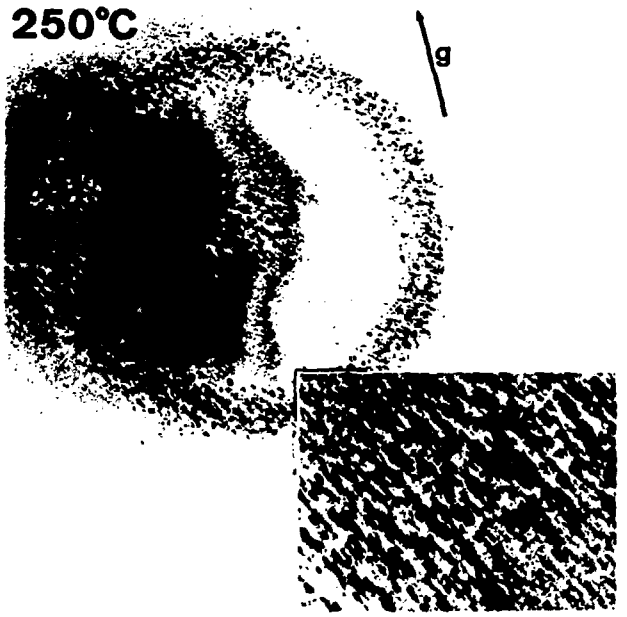

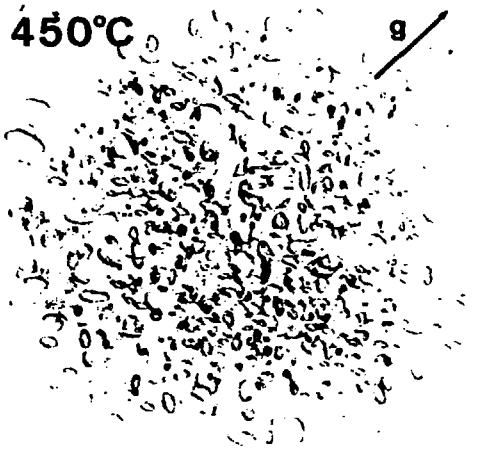

3 μm

$\underline{g}$ = <110>
$\underline{z}$ ~ <111>

HELIUM EFFECTS: CAVITIES

Fe:

- CAVITIES WERE FOUND IN HALOS FORMED AT 650°C, WHILE NO CAVITIES WERE FOUND IN NONHALO REGIONS.
- NEAR THE HALOS, CAVITIES FORMED ON AND NEAR GRAIN BOUNDARIES.

3 μm

650°C

600 nm

HELIUM EFFECTS: CAVITIES

V:

- THE V-B_4C SPECIMENS CONTAINED HIGHER CONCENTRATIONS OF SMALLER CAVITIES AND EXHIBITED MORE EXTENSIVE CAVITY FORMATION AT HIGHER IRRADIATION TEMPERATURES THAN DID VANADIUM.
- THE SWELLING IN V-B_4C IS HIGHER THAN THE SWELLING IN V.
- CAVITIES WERE OBSERVED ON GRAIN BOUNDARIES IN V-B_4C.

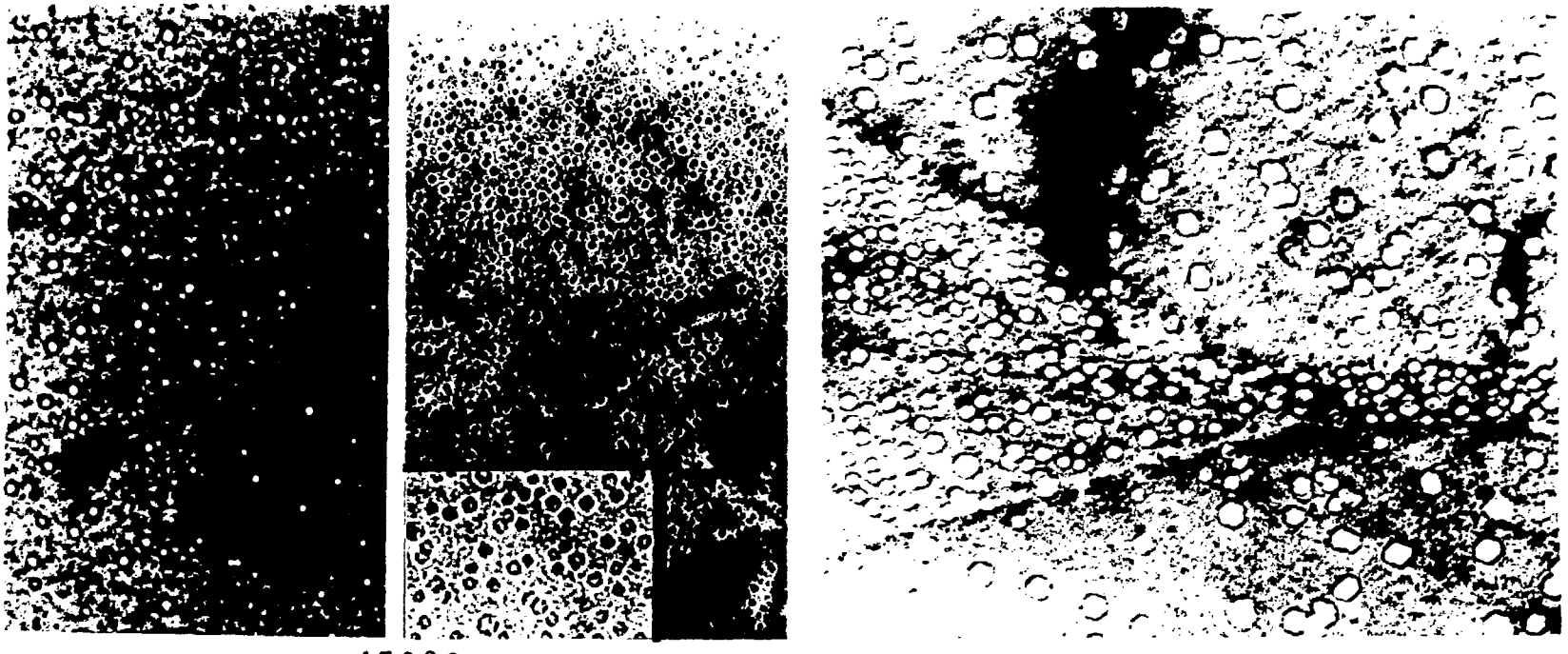

Vanadium 450°C 100 nm V-B_4C V-B_4C 650°C 100 nm

ORNL-DWG 83-19011

COMPARISON OF NUMERICAL CAVITY DATA: V, V-B_4C

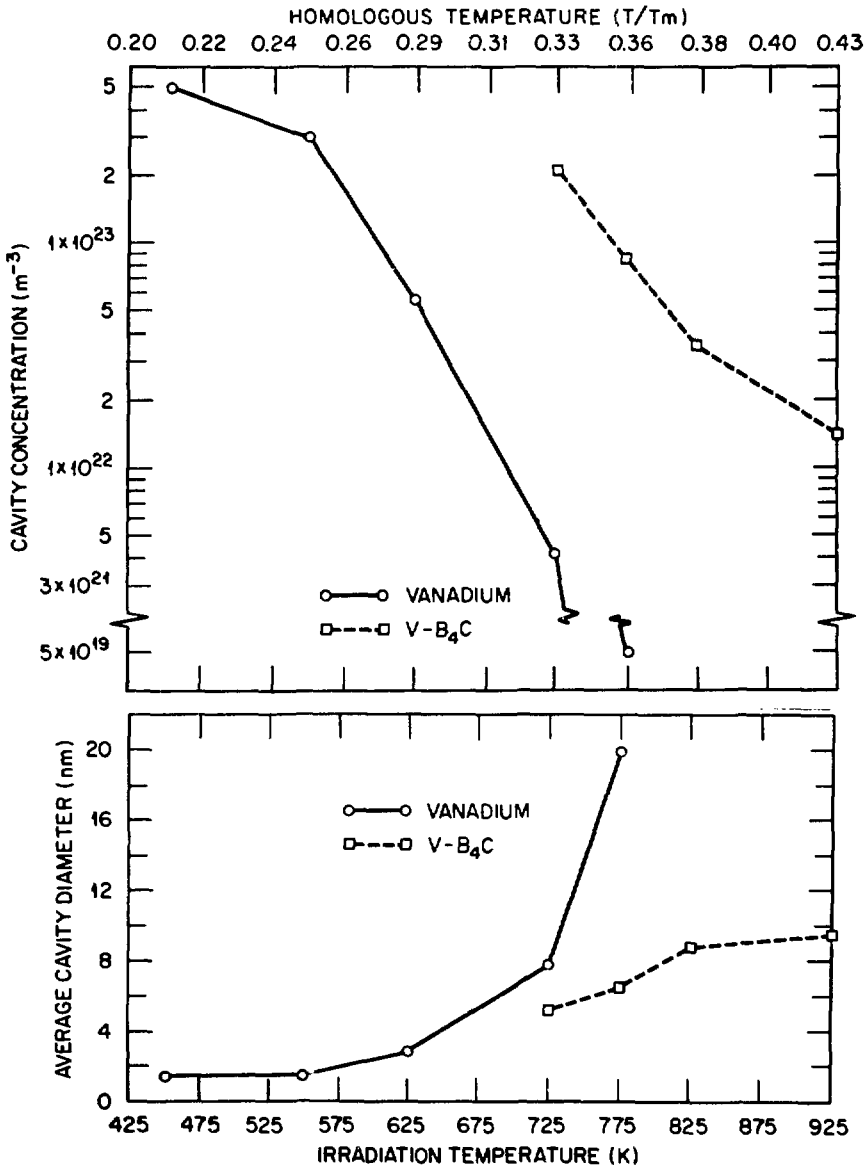

ORNL-DWG 83-19012

COMPARISON OF NUMERICAL CAVITY DATA: V, V-B_4C

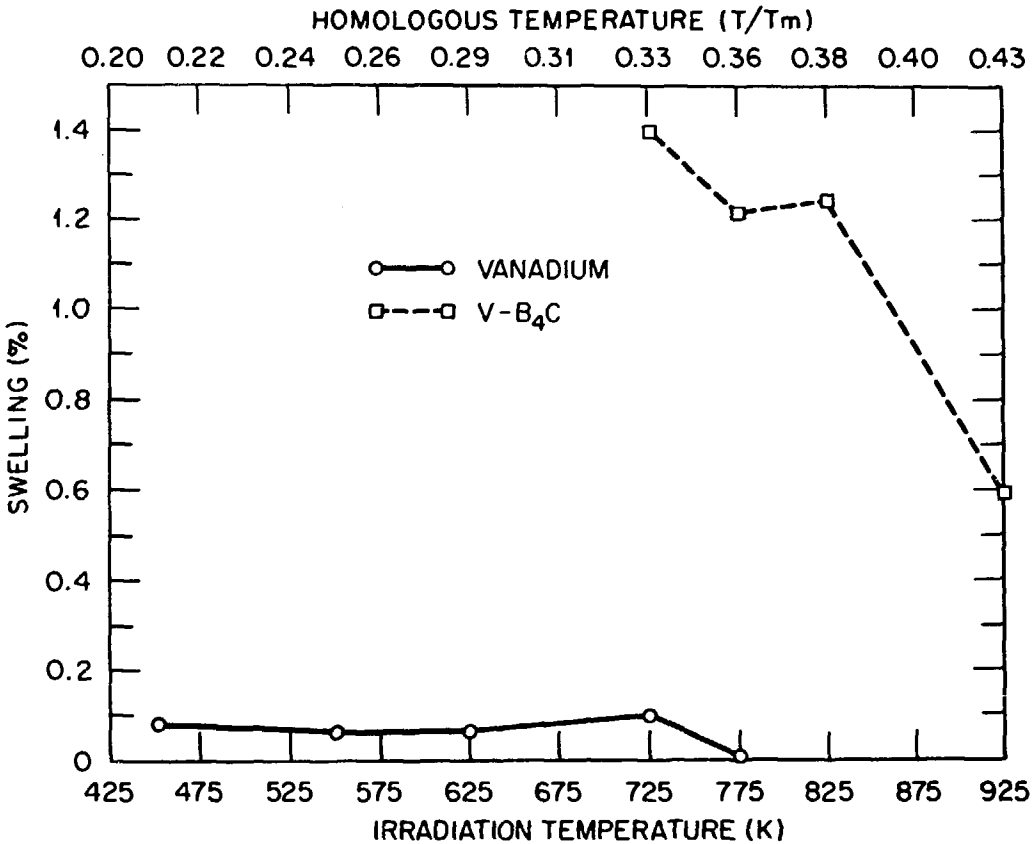

ORNL-DWG 83-18909

COMPARISON OF NUMERICAL CAVITY DATA: V, Fe

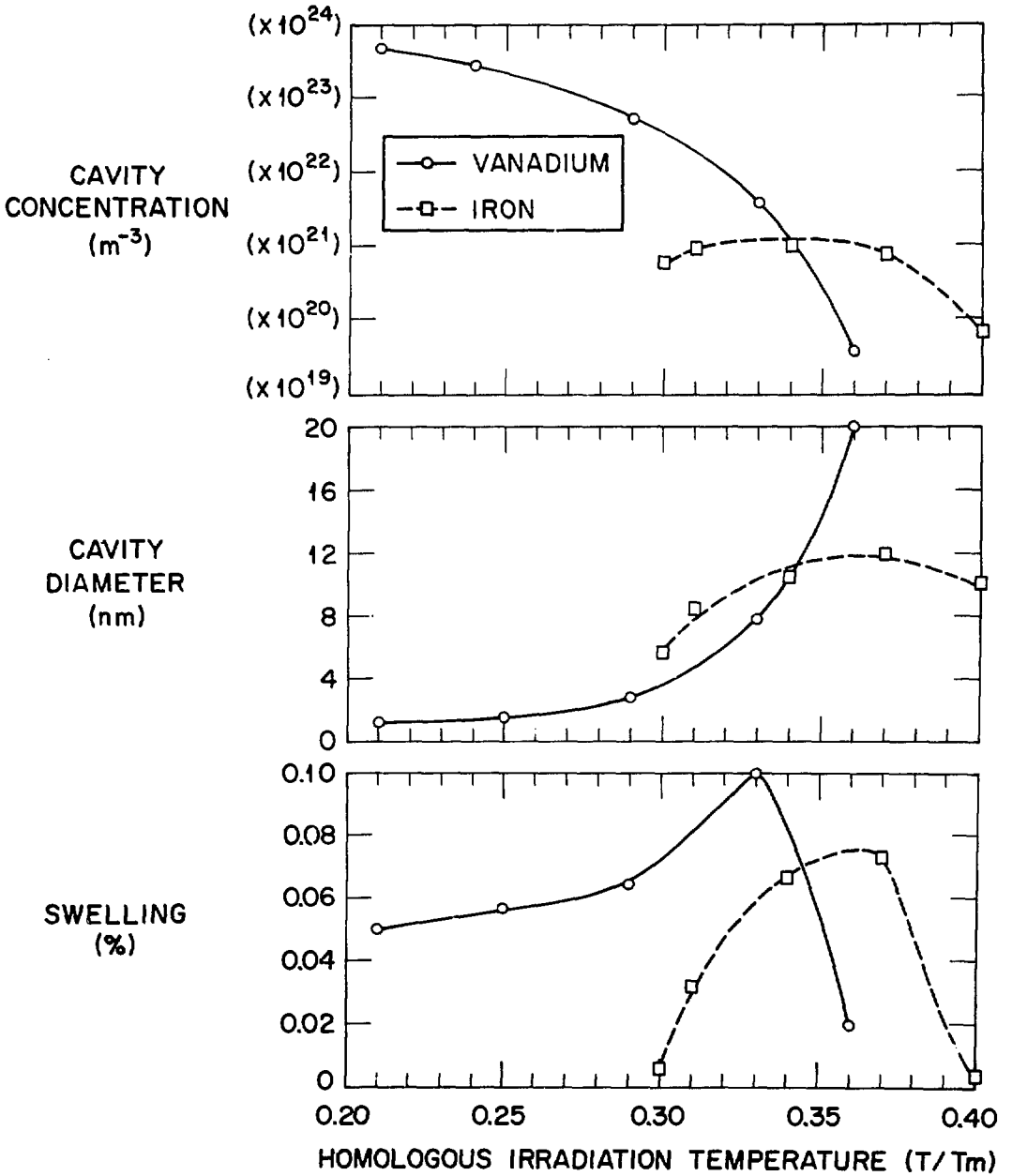

ORNL-DWG 83-18627R1

COMPARISON OF CAVITY MICROSTRUCTURES: V, Fe

Fe:

- SIGNIFICANT CAVITY FORMATION IS LIMITED TO 0.30–0.40 T_m (275–450°C)
- HOMOGENEOUS DISTRIBUTION OCCURRED ONLY AT 0.34 and 0.37 T_m (350,450°C)
- THE CAVITIES HAVE A TRUNCATED OCTAHEDRAL SHAPE WITH {111} FACES AND {100} TRUNCATIONS.
- MAXIMUM SWELLING OF ~0.07% OCCURRED AT 0.34–0.37 T_m.

V:

- CAVITIES WERE OBSERVED FOR ALL IRRADIATION TEMPERATURES (0.21–0.36 T_m).
- INHOMOGENEOUS DISTRIBUTIONS OCCURRED ONLY AT HIGHEST IRRADIATION TEMPERATURE, 0.36 T_m (500°C).
- NO DISTINCT FACETS WERE OBSERVED.
- MAXIMUM SWELLING OF ~0.1% OCCURRED AT 0.33 T_m.

IN GENERAL, FOR THE SAME HOMOLOGOUS TEMPERATURE, THE CAVITIES WERE SMALLER, WERE PRESENT IN HIGHER CONCENTRATIONS, AND CAUSED LARGER SWELLING FOR VANADIUM THAN FOR IRON.

ORNL-DWG 83-18628

THESE RESULTS ARE FURTHER EVIDENCE THAT THE DAMAGE MICROSTRUCTURES FOR FERRITIC MATERIALS DIFFER FROM THOSE FOR OTHER bcc MATERIALS

- IRON WAS MORE RESISTANT TO SWELLING THAN WAS VANADIUM
- CAVITY MORPHOLOGY:

  Fe - TRUNCATED OCTAHEDRON {111} faces, {100} truncations

  V-B_4C - TRUNCATED DODECAHEDRON, {110} faces, {100} truncations
- DISLOCATION LOOP BURGERS VECTORS:

  Fe - a<100>

  V - a/2<111>

THE EFFECTS OF HELIUM PRODUCED FROM $^{10}B(n,\alpha)^{7}Li$ REACTIONS INCLUDE:

- HIGHER DISLOCATION DENSITIES (Fe) AND HIGHER CONCENTRATION OF SMALLER CAVITIES (V)
- CAVITY FORMATION ON gbs (Fe, V)
- CAVITY FORMATION AT HIGHER IRRADIATION TEMPERATURE IN V-B_4V THAN V

- Pulsed Irradiation Effects in a Stable Austenitic Alloy

ORNL-DWG 83-19017

PULSED ION IRRADIATIONS OF A "PURE" STAINLESS STEEL

IRRADIATIONS CARRIED OUT AT 843, 938, AND 1023 K TO 10 dpa.

CONDITIONS: SIMULTANEOUS He, PREIMPLANTED He, NO He

PULSING CONDITIONS: "FAST" (1s ON/1s OFF)
"SLOW" (60s ON/60s OFF), CONTINUOUS

MOST SIGNIFICANT PULSING EFFECTS

AT 938 K PULSING SEEMED TO PREVENT THE USUAL REFINEMENT OF CAVITIES CAUSED BY HELIUM INJECTION.

AT 1023 K, NEAR THE HIGH TEMPERATURE LIMIT FOR SWELLING, PULSING SUPPRESSED ALL LARGE CAVITIES.

938 K

CONTINUOUS | SLOW PULSE

NO HELIUM

DUAL BEAM

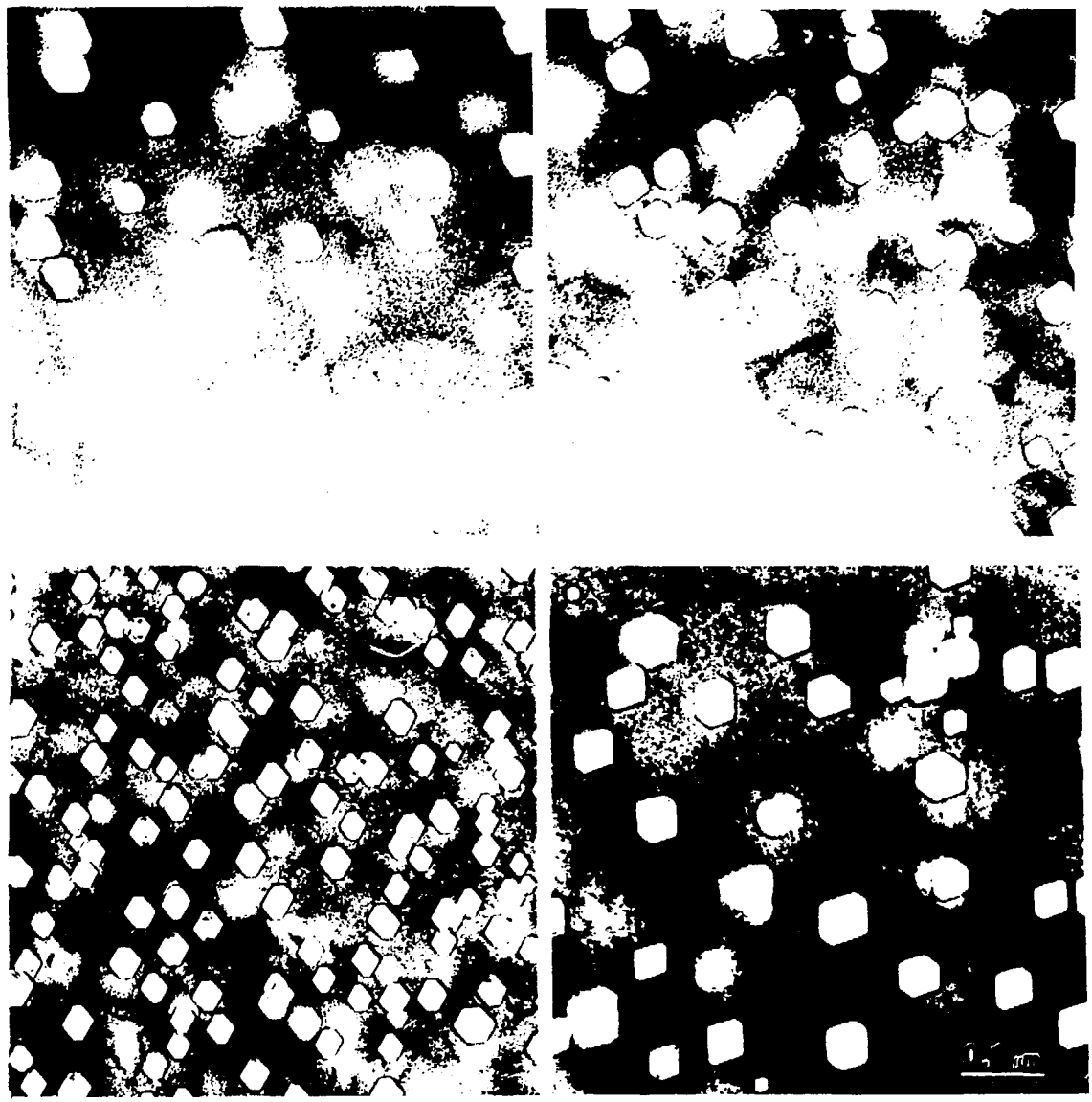

1023 K

CONTINUOUS

SLOW PULSE

NO HELIUM

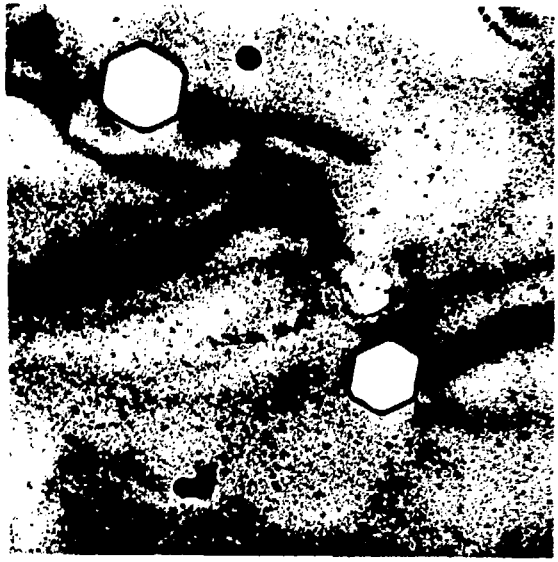

DUAL BEAM

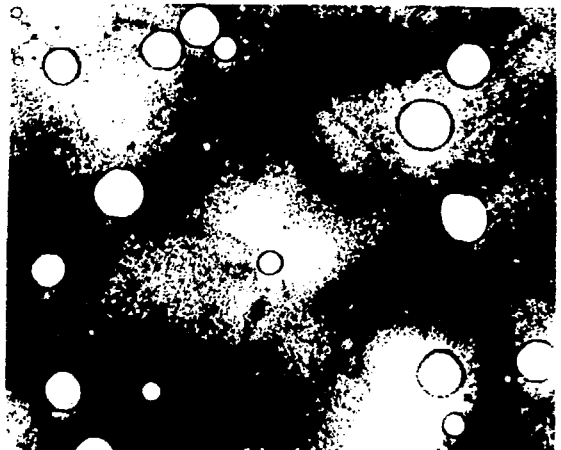

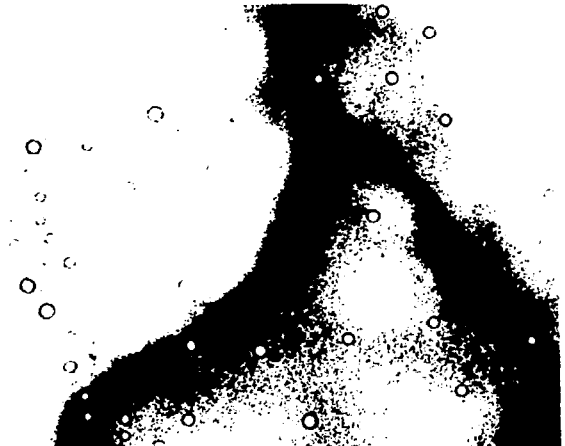

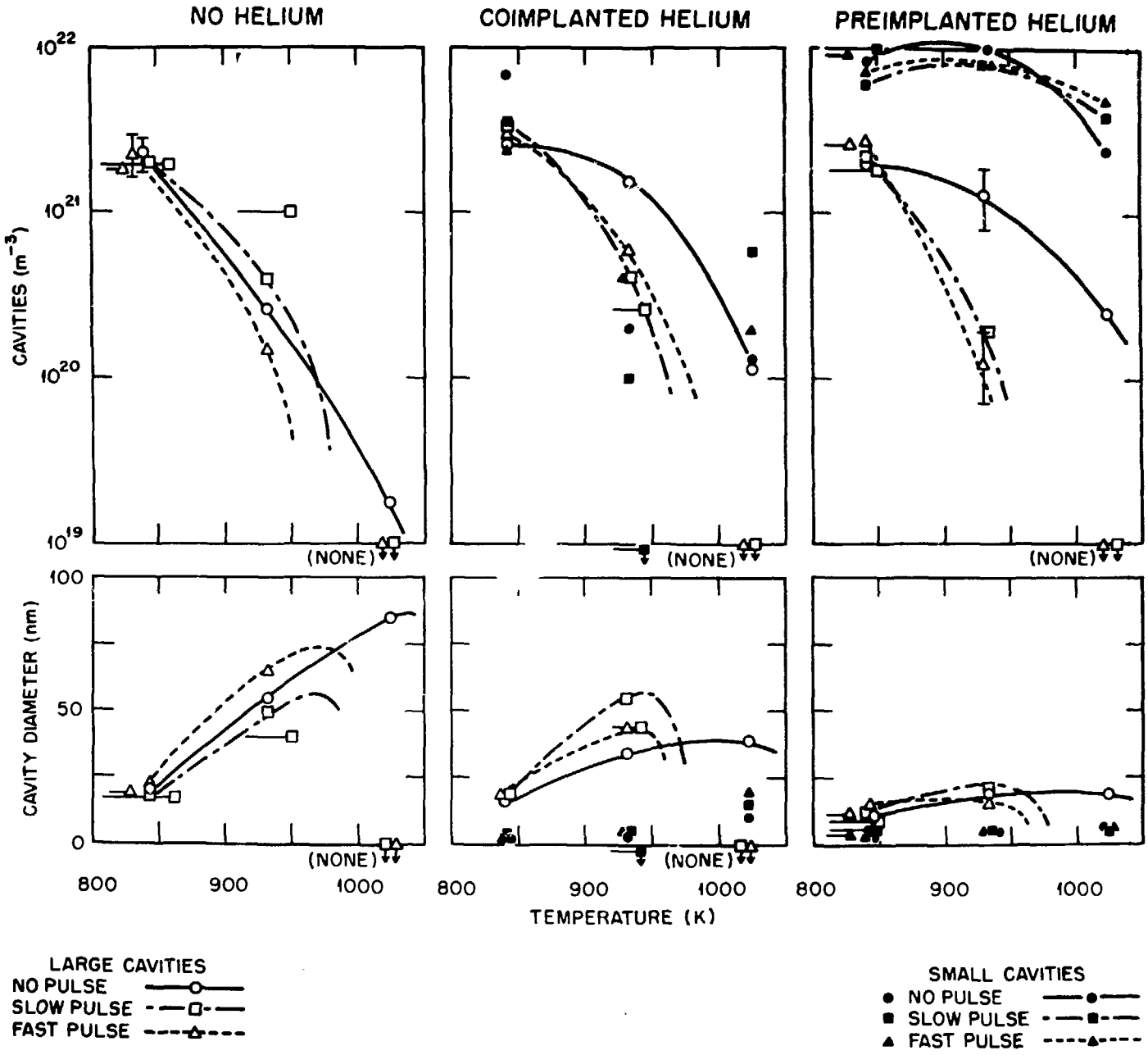
NO HELIUM
COIMPLANTED HELIUM
PREIMPLANTED HELIUM
CAVITIES (m^{-3})
10^{22}
10^{21}
10^{20}
10^{19}
(NONE)
CAVITY DIAMETER (nm)
100
50
0
800
900
1000
TEMPERATURE (K)
LARGE CAVITIES
NO PULSE
SLOW PULSE
FAST PULSE
SMALL CAVITIES
NO PULSE
SLOW PULSE
FAST PULSE

ORNL-DWG 83-19015

THE MECHANISM OF SUPPRESSION OF SWELLING AT HIGHER TEMPERATURES BY PUSLING CAN BE UNDERSTOOD AS AN EFFECT OF INTERMITTENT ANNEALING

ALLOWS CAVITIES TO SHRINK BY THERMAL ANNEALING

STABLE SIZE IS SOMEWHAT SMALLER FOR PULSED IRRADIATIONS BECAUSE OF THERMAL ANNEALS.

HELIUM MIGRATION MAY BE AFFECTED BY WHETHER OR NOT POINT DEFECT PRODUCTION IS OCCURRING.

- Pulsed Irradiation Effects in an Unstable Austenitic Alloy

ORNL-DWG 83-18619

OBSERVED EFFECTS OF PULSING ON MICROSTRUCTURE AND PRECIPITATION

- LOOP SIZE IS DECREASED BY PULSING.
- MC STABILITY IS INCREASED BY PULSING.
- CAVITIES DID NOT FORM IN THE ABSENCE OF HELIUM WITH OR WITHOUT PULSING.
- MAJOR PHASES ARE G AND MC.

ORNL-DWG 83-18620

OBSERVED EFFECTS OF PULSING AND SIMULTANEOUS HELIUM INJECTION ON MICROSTRUCTURAL AND PHASE STABILITY

- LOOP SIZE IS DECREASED FURTHER BY HELIUM INJECTION.
- MC STABILITY IS INCREASED BY HELIUM INJECTION.
- CAVITY FORMATION IS RETARDED BY PULSING.
- η (LOWER Si and Ni) PHASE FORMS INSTEAD OF G PHASE WHEN BOTH He INJECTION AND PULSING ARE APPLIED.

ORNL-PHOTO 3641-82

ORNL-PHOTO 3642A-82

PULSED ION IRRADIATION WITH SIMULTANEOUS HELIUM INJECTION LEADS TO LARGE CHANGES IN SWELLING, PHASE TRANSFORMATIONS AND DISLOCATION LOOPS

ORNL–DWG 82-18624

EFFECT OF PULSING AND HELIUM INJECTION ON CAVITY GROWTH

NO HELIUM, CONTINUOUS

HELIUM, CONTINUOUS

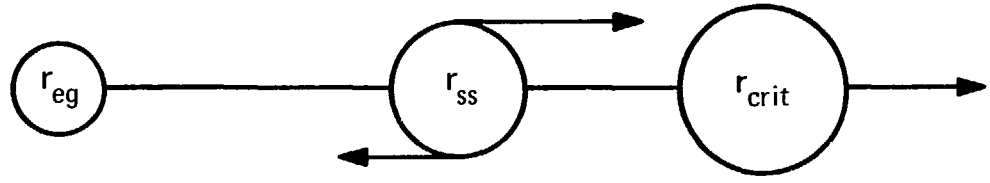

HELIUM, PULSED

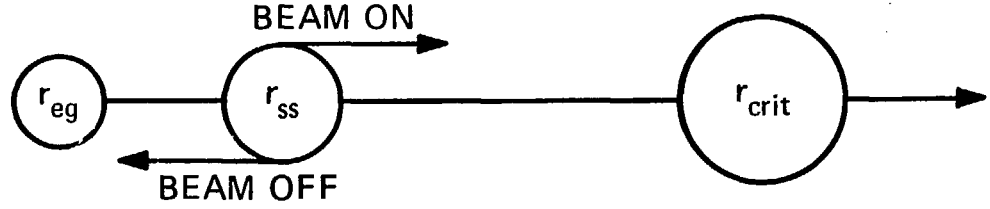

ORNL-DWG 83-18622

EFFECT OF PULSING AND HELIUM INJECTION ON PHASE STABILITY

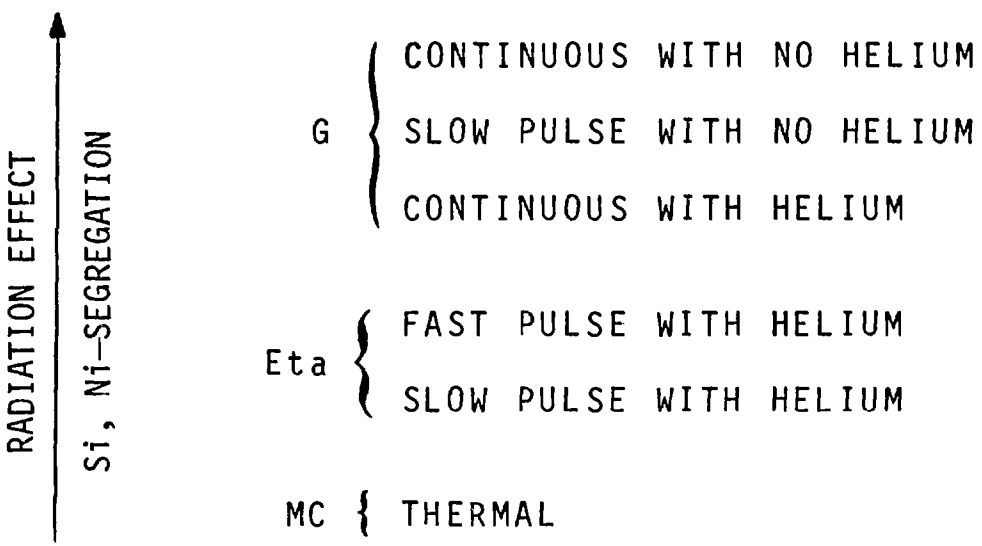

- He REDUCES RIS EFFECT BY SOLUTE DILUTION ON THE HIGH DENSITY OF CAVITIES.
- PULSING REDUCES RIS EFFECT BY THERMAL RELAXATION OF RIS PROFILES.
- Eta PHASE REQUIRES LESS Si AND Ni SEGREGATION AND THEREFORE FORMS INSTEAD OF G-PHASE UNDER PULSING WITH HELIUM INJECTION.